

Reactive compatibilisation of heterogeneous ethylene propylene rubber (EPM)/nylon 6 blends by the addition of compatibiliser precursor EPM-g-MA

Sabu Thomas^{1,*}, G. Groeninckx

Laboratory of Macromolecular Structural Chemistry, Department of Chemistry, Katholieke Universiteit Leuven (KULeuven), Celestijnenlaan 200F, B-3001 Leuven (Heverlee), Belgium

Received 24 August 1998; received in revised form 18 November 1998; accepted 18 November 1998

Abstract

Blends of ethylene-propylene rubber (EPM) and nylon 6 are immiscible and highly incompatible. These blends are characterised by a two-phase morphology, narrow interface, and poor physical and chemical interactions across the phase boundaries. Therefore a reactive route was employed to compatibilise these blends by the addition of maleic anhydride grafted EPM (EPM-g-MA). In this reactive route, the maleic anhydride group of EPM reacts with the amino end group of nylon forming a graft copolymer of nylon and EPM (nylon-g-EPM) at the blend interface which decreases the interfacial tension and reduces the coalescence. The influence of the concentration of EPM-g-MA, blend composition, molecular weight of nylon 6, mode of addition of EPM-g-MA and mixing time on the phase morphology of the blends was studied quantitatively by scanning electron microscopy and image analysis. It was found that the addition of EPM-g-MA reduces the domain size of the dispersed phase followed by a levelling off at high concentrations; the levelling off is an indication of interfacial saturation. The optimum amount of the compatibiliser required to saturate unit volume of the interfacial zone was estimated from the emulsification curves. This optimum concentration of the compatibiliser can be considered as the so-called critical micelle concentration (CMC) above which micelles of the copolymer are formed in the bulk phase, which is highly undesirable. Emulsification master curves were obtained by plotting the reduced domain size as a function of EPM-g-MA for the different blend compositions. This was explained based on the interfacial area occupied by the compatibiliser molecule at the blend interface. The experimental results were compared with the current compatibilisation theories. The phase morphology development was studied as a function of the mixing time in the presence and absence of compatibiliser. The influence of reactive compatibilisation on phase inversion and the co-continuous nature of the blends was also investigated. Finally the stability of the blend morphology was analysed by high temperature isothermal annealing in the presence and absence of compatibiliser
© 1999 Elsevier Science Ltd. All rights reserved.

Keywords: EPM; Nylon 6; Compatibilisation

1. Introduction

The concept of physically combining two or more polymers via blending to obtain new polymeric materials with the desired properties has received lot of attention from the point of view of fundamental and practical interests. In fact blending of polymers is, in principle, one of the easiest and most flexible methods to generate new polymeric materials. The alternative to blending is synthesising new polymers which not only involves exorbitant costs but also cannot always fulfil end use requirements. When two or

more polymers are mixed, the phase structure of the resulting material can be either miscible, partially miscible or immiscible. As a result of their high molar mass, the entropy of mixing of polymers is relatively low and consequently specific interactions are needed to obtain blends which are miscible or homogeneous on a molecular scale. For this reason, the number of miscible polymer pairs is relatively limited. In the case of immiscible pairs, homogeneous mixing on a molecular scale cannot be obtained and a heterogeneous blend results after mixing. Among the different types of polymer blends, thermoplastic elastomers (TPEs) from rubber/thermoplastic blends have gained lot of interest recently as they bridge the gap between thermoplastics and elastomers [1,2]. However, most of the TPEs from rubber/thermoplastic blends are immiscible and incompatible.

* Corresponding author.

¹ Permanent Address: School of Chemical Sciences, Mahatma Gandhi University, Priyadarshini Hills PO Kottayam, Kerala, India 686 560.

E-mail address: mgu@md2.vsnl.net.in (S. Thomas)

Table 1
Properties of component polymers used

Polymer	Source	M_w
Ethylene–propylene rubber (EPM) (78% ethylene content)	Exxon	80 000
Ethylene–propylene rubber-g-maleic anhydride(EPM-g-MA, 0.6 wt.%MA)	Exxon	80 000
Polyamide 6	DSM	15 000
Polyamide 6	DSM	24 000
Polyamide 6	DSM	34 000
Polyamide 6	DSM	44 000

Usually a high interfacial tension between the phases of an immiscible polymer blend leads to coarse and unstable morphologies. In addition, a high interfacial tension results in a narrow interface, poor physical and chemical interactions across the phase boundaries, and as a consequence, in a poor adhesion between the phases. For blend systems the mechanical behaviour depends critically on two demanding structural parameters, a proper interfacial tension leading to a phase size small enough to allow the material to be considered as macroscopically homogeneous, and an interface adhesion strong enough to assimilate stresses and strains without disruption of the established morphology. This can be achieved by different ways [3–6]. One way is to organise the phases so as to increase the interfacial area so that the components will be able to transfer the applied stress effectively despite having high interfacial tension. Techniques of blending have been used successfully in some blend systems to form interpenetrating co-continuous network phases. Such systems have improved mechanical properties because of the continuous nature of the phases which allows direct load sharing between the components without the need for stress transfer across the phase boundaries. However, this is not successful in all cases.

It is now well established that the phase morphology of immiscible polymer blends can be controlled by the addition or the in-situ formation of compatibilisers (block or graft copolymers) which act as interfacial agents. The addition of a suitably selected compatibiliser to an immiscible binary blend should (i) reduce the interfacial energy between the phases, (ii) permit finer dispersion during melt-mixing (iii) provide stability against gross segregation and (iv) result in improved interfacial adhesion [3]. Several experimental investigations have been reported on the compatibilising action of added block and graft copolymers in heterogeneous polymer blends (physical compatibilisation). The pioneering studies in this area have been reported by Molau [7], Riess et al. [8], Teyssié et al. [9], Heikens et al. [10] and Paul et al. [11].

In recent years, more attention has been focused on reactive compatibilisation of immiscible polymer blends giving rise to in-situ generation of copolymers. This is a very fast, easy, and cost effective alternative. The basic principle underlying reactive compatibilisation is that by making

use of the functionalities present in one or more polymers, one can form graft or block copolymers in-situ during melt-processing. These in-situ formed copolymers act as compatibilisers by reducing the interfacial tension and increasing the adhesion between the phases, and thereby allowing a finer dispersion and a more stable morphology. This method has been applied to a number of blend systems such as polyamide/polyolefins, polyamide/ABS, PS/polyolefins, polyester/polyamide, polyamide/polyamide, and various rubber/plastic blends [12–19]. Several review articles have appeared in the literature emphasising the importance and potentialities of blend compatibilisation using reactive polymer processing [20,21]. Different types of chemical reactions can be used in compatibilising polymer blends; reactions as imidization, esterification, amidation, aminolysis, ester–ester interchange, amide–ester interchange, ring opening and ionic bonding can occur rapidly at elevated processing temperatures [21].

Blends of nylon 6 and EPM are highly immiscible and incompatible. This is because of the fact that the interfacial tension between the two polymers is extremely high on account of the high polarity difference. Although several studies have been reported [22–25] on the morphology and compatibilisation of these blends, detailed investigations relating the compatibilising efficiency to the concentration of the functionalised polymer (EPM-g-MA), molecular weight of the component homopolymers and mode of addition of the modified polymer are lacking. Also, the influence of reactive compatibilisation on the stability of the blend morphology has not been well understood. The purpose of the present study is to analyse quantitatively the effect of concentration of EPM-g-MA on the phase morphology of EPM/nylon 6 blends as a function of composition, processing conditions and molecular weight of the nylon phase. The experimental results were compared with theoretical predictions. The stability of the blends was analysed by isothermal annealing of the blends at high temperature in the melt. The morphology development as a function of mixing time was studied in the presence and absence of compatibiliser. The morphology was studied by scanning electron microscopic examination of the preferentially extracted (EPM or nylon depending on the composition) blend samples. The micrographs were quantitatively analysed by image analysis. Finally, the extent of interfacial bonding in these blends was evaluated in the presence and absence of compatibiliser by the examination of the fracture surfaces using SEM.

2. Experimental

2.1. Materials

The characteristics of the EPM rubber, EPM-g-MA and different types of nylon 6 used in this study are given in Table 1. Both EPM rubber and nylon 6 are commercially

Table 2
Apparent viscosities (Pa S) of EPM and Nylon 6 ($M_w = 24,000$) at 250°C

Shear Rate (s^{-1})	η_{EPM}	η_{nylon}	η_{EPM}/η_{nylon}
5	6410	1643	3.90
10	4955	1381	3.61
20	4143	1259	3.29
30	3669	1223	3.06
50	3045	1091	2.79
100	2296	952	2.41
200	1583	802	1.97

available. Nylon 6 of varying molecular weight was received from DSM. The EPM and EPM-g-MA rubber were supplied by Exxon Chemical Company. All the nylons were dried at 120°C for 12 h prior to blending. For all the experiments, except the study related to the molecular weight of nylon, nylon 6 of molecular weight (M_w) 24 000 was used. The apparent melt viscosity of EPM and nylon 6 were determined in a Gottfert 2002 Rheometer at 250°C. The viscosity values are given in Table 2 as a function of shear rate.

2.2. Melt blending

Blends were prepared in a co-rotating conical twin-screw batch type mini-extruder (DSM) under nitrogen atmosphere. All the components (EPM, nylon 6 and EPM-g-MA) were fed into the extruder simultaneously unless otherwise specified. The mixing time, temperature and rotor speed were 10 min, 250°C and 100 rpm, respectively. However, in order to study the influence of the mixing time on blend phase morphology, experiments were performed as a function of time of mixing at constant rotor speed (100 rpm) and temperature (250°C).

2.3. Phase morphology studies

A scanning electron microscope was used to examine the phase morphology of the blends. The samples were fractured under liquid nitrogen and one of the phases was

preferentially extracted. For blend samples having dispersed EPM phase, this phase was extracted by using boiling xylene for 12 h. The EPM phase was also extracted in blends having co-continuous morphologies (50/50 and 60/40 EPM/nylon). When the nylon is the dispersed phase, this phase was removed by using formic acid at ambient temperature for a period of 12 h. The dried samples were sputter coated with gold prior to SEM examination. A Philips scanning electron microscope operating at 10 KV was used. Several micrographs were taken for each sample. In order to analyse the extent of interfacial bonding, cryogenically fractured surfaces of the samples were analysed by SEM.

The dispersed phase size analysis was done using an automatic image analysing technique which employed an IMAGE software. The apparent diameter was measured by scanning the micrographs and individually outlining the particles to calculate their dimensions. Typically over 400 particles and several fields of view were analysed. The number average diameter (D_n) and weight average diameter (D_w) were calculated from the following relationships:

$$D_n = \frac{\sum n_i D_i}{\sum n_i} \quad (1)$$

$$D_w = \frac{\sum n_i D_i^2}{\sum n_i D_i} \quad (2)$$

where n_i is the number of particles with diameter D_i .

3. Results and discussion

3.1. Rheology of EPM rubber and nylon 6

The rheological behaviour of the component polymers nylon 6 ($M_w = 24,000$) and EPM rubber at a temperature of 250°C as a function of shear rate is given in Table 2. It can be seen that the melt-viscosity of EPM rubber is much higher than that of nylon over the entire range of shear rate studied. At the very low shear rate region ($5 s^{-1}$), the viscosity of EPM is four times higher than that of nylon. At the higher shear rate region ($200 s^{-1}$), the viscosity of EPM is two times higher than that of nylon. The viscosity ratios of

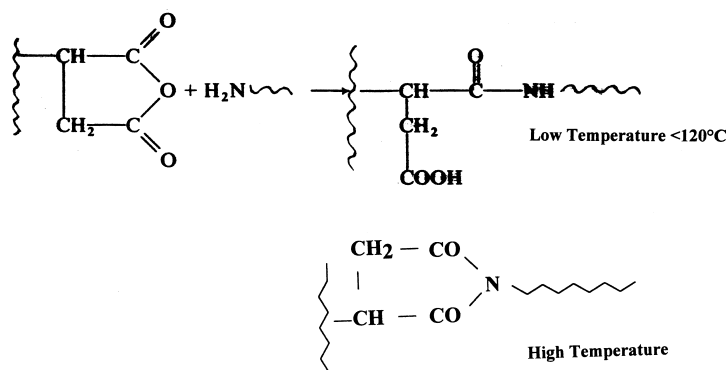


Fig. 1. Compatibilisation strategy, reaction between amine end group of nylon and anhydride group of EPM-g-MA leading to the formation of amide or imide linkages.

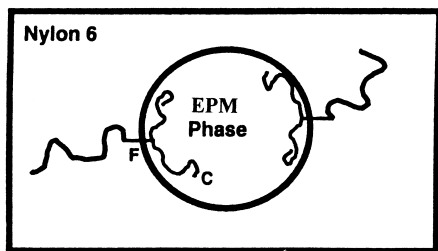


Fig. 2. Schematic model illustrating the location of the graft copolymer at the blend interface.

the components ($\eta_{\text{EPM}}/\eta_{\text{nylon}}$) decrease with increasing shear rate. As expected, the viscosity of the polymers decreases with increasing shear rate indicating their pseudoplastic nature. In fact EPM is more pseudoplastic than nylon as the decrease of viscosity with increase of shear rate is more predominant in the case of EPM.

3.2. Compatibilisation strategy

Polyamides represent an important class of engineering thermoplastics which find lots applications. However, they exhibit certain inherent deficiencies. These include brittleness, high moisture absorption, poor dimensional stability and marginal heat deflection temperature. Several studies have reported how to alleviate this problem by reactive blending with other polymers [20,21]. Most of these studies are based on the fact that nylons have inherent chemical functionalities (amine and carboxyl end groups and potential amide linkages) which are capable of reacting with the functional groups present in the second polymer with which it is blended.

The present compatibilisation strategy involves the compatibilisation of nylon 6 with a second immiscible phase (EPM rubber) by the introduction of a compatibiliser precursor (EPM-g-MA) which is physically miscible with the second phase but has chemical functionality (maleic anhydride group) which can react with the amino end group of nylon to form a graft copolymer at the interface as shown in Fig. 1. The idealised location of the graft copolymer is demonstrated in Fig. 2 where the compatibiliser species C is miscible with the EPM phase and has functional groups F which are capable of forming linkages with the nylon chains at the interface. This situation is expected to lead to a reduction in particle size through a reduction in interfacial tension and an increased resistance to coalescence through stabilisation of the interface.

In fact the reaction between nylon 6 and maleic anhydride modified polyolefin polymers and the subsequent graft copolymer formation have been well documented in literature. This reaction was first reported by Ide and Hasegawa [12]. They studied the blends of nylon 6 and polypropylene to which maleic anhydride modified polypropylene was added to improve the dispersability and mechanical behaviour of the two immiscible polymers. The existence of such a graft copolymer was confirmed by solvent extraction,

estimation of the amino end groups of nylon 6, and identification by differential scanning calorimetry. Martuscelli and co-workers [14,22,23] have reported that the grafted anhydride groups can be transformed to acid, ester, and amide (or imide) groups by reaction with water, alcohols, and amines, respectively. The authors further reported that reaction of EPM-g-MA with the aliphatic amines such as *n*-hexylamine leads to amidic or imidic linkages according to the reaction temperature. At low temperature ($T < 120^\circ\text{C}$), amidic linkages are reported to be prevalent, whereas at high temperature, almost only imidic bonds are present as revealed by IR analysis. They have considered the above reaction as the as model scale reaction that occurs between the melt blending of nylon 6 and EPM-g-MA at 260°C indicating that likely imide linkages are present in the EPM-g-nylon 6 copolymer formed during the reaction. It is also important to add that one must consider the possibility of graft copolymer formation by the breaking of amide bonds of nylon 6 by means of anhydride or carboxylic groups of the functionalised EPM. Very recently, the structure of EPDM grafted to nylon 66 has been analysed with high resolution solid state ^{13}C NMR and IR spectroscopy by van der Velden et al. [26].

3.3. Effect of blend composition and mixing time on phase morphology development

The properties of polymer blends are strongly influenced by their morphology. The morphology of heterogeneous polymer blends in general depends on blend composition, interfacial tension between the component polymers, viscosity ratio and processing history. Therefore it is important to study the relationship between processing conditions, blend composition and the final blend phase morphology.

The main mechanism governing the morphology development is believed to be the result of both droplet break-up and coalescence. The pioneering work of Taylor on drop break-up in Newtonian systems in a simple shear field has been the basis of the investigations on more complex systems and flow fields [27,28]. The analysis of Taylor considers how the balance of applied shear forces and the counteracting interfacial forces affects drop dimensions and stability. The results have been expressed in terms of the so-called well known capillary number,

$$\text{Ca} = \dot{\gamma}\eta_m D/2Y \quad (3)$$

and the viscosity ratio, $\eta_r = \eta_d/\eta_m$, where D is the diameter of the droplet, $\dot{\gamma}$ the shear rate, η_m the matrix viscosity, η_d the dispersed phase viscosity, and Y the interfacial tension. Drop break-up is predicted to occur when the viscosity ratio is less than 2.5. Interestingly, several studies on Newtonian systems in both shear and extensional flow were in agreement with Taylor's predictions [29–33]. However, it has been reported that drop break-up was possible over a wide range of viscosity ratios in extensional flow for Newtonian systems [34–38]. In the case of viscoelastic systems like

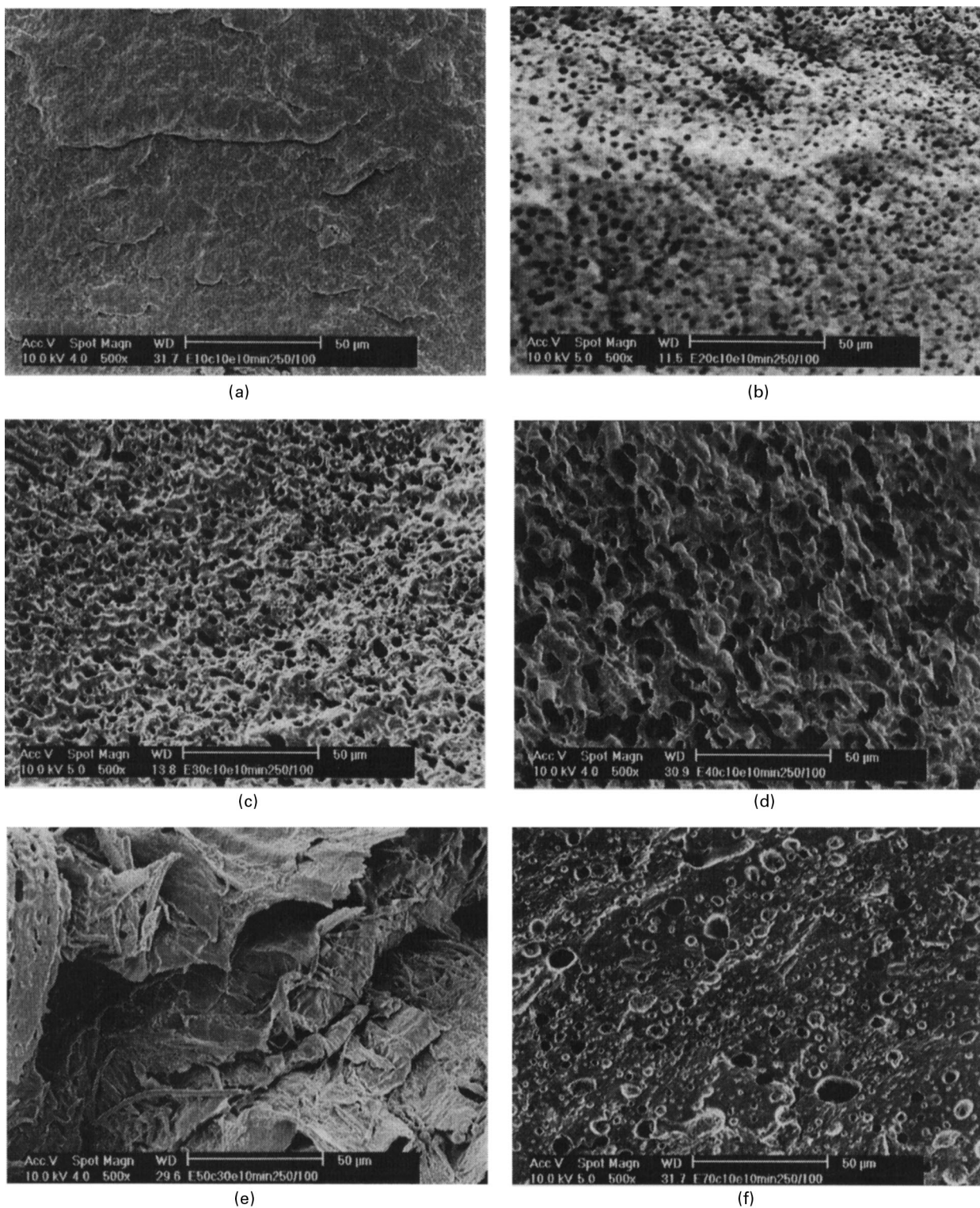


Fig. 3. SEM micrographs showing the morphology of reactively compatibilised EPM/nylon blends containing 10 wt.% of EPM-g-MA: (a) 10/90 EPM/nylon blend; EPM is dispersed as domains in the continuous nylon matrix, (b) 20/80 EPM/nylon blend; EPM is dispersed as domains in the continuous nylon matrix, (c) 30/70 EPM/nylon blend; EPM is dispersed as domains in the continuous nylon matrix, (d) 40/60 EPM/nylon blend; EPM is dispersed as domains in the continuous nylon matrix, (e) 50/50 EPM/nylon blend; interpenetrating co-continuous morphology, (f) 70/30 EPM/nylon blend; nylon is dispersed as domains in the EPM matrix, (g) 80/20 EPM/nylon blend; nylon is dispersed as domains in the continuous EPM matrix, (h) 90/10 EPM/nylon blend; nylon is dispersed as domains in the continuous EPM matrix.

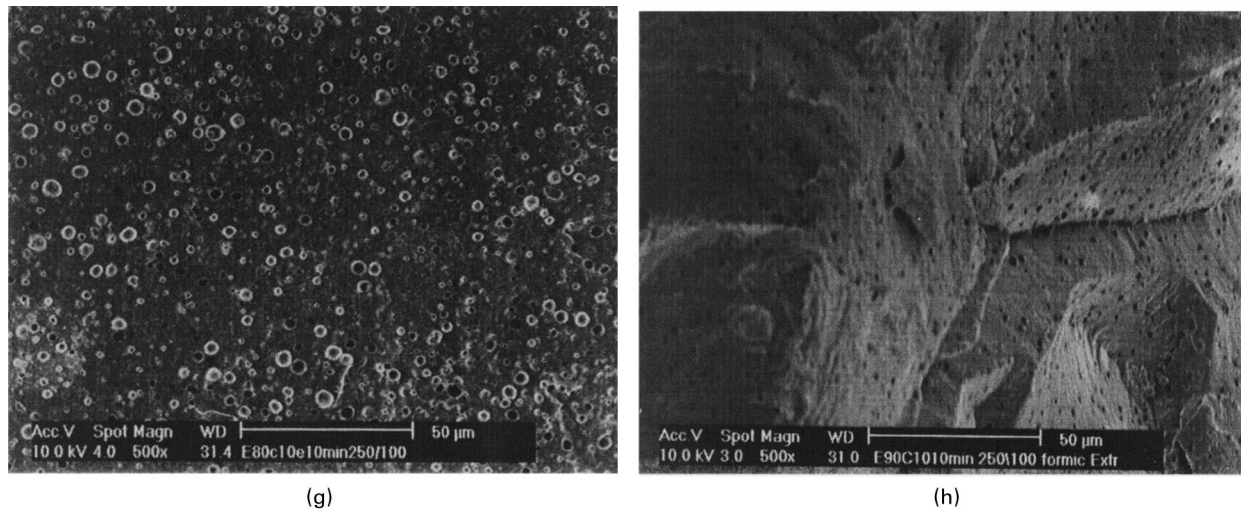


Fig. 3. (continued)

polymer blends, as the individual components exhibit large normal stresses in flow, the extension of Taylor's analysis to such systems has some limitations. It is also important to add that the final morphology of polymer blends is the result of the balance of domain break-up and coalescence at the end of the mixing process. However, most of the studies on polymer blends in literature regarding domain size, expressed in terms of capillary number and viscosity ratio (based on Taylor's analysis), do not account for the coalescence process. In one of the most interesting and frequently cited studies on nylon/rubber blends, Wu extrapolated an empirical equation fitting the capillary master curve[39]. According to this equation,

$$\dot{\gamma} \eta_m D / Y = 4(\eta_r)^{\pm 0.84}. \quad (4)$$

Wu's correlation suggests a minimum particle size when the viscosities of the two phases are closely matched. The validity of this equation has been testified by several researchers. Utracki and co-workers [40], Roland and Bohm [41], and Paul and co-workers [42] have indicated some disagreement with respect to the dependence of particle size and viscosity ratio and the correlation proposed by Wu. In contrast, Serpe et al. [43] found good agreement with Wu's results in their experimental observations. Recently Sundararaj and Macosko [5] have reported on the experimental minimum in the dispersed phase size with increasing shear rate; they have explained this behaviour based on the high elasticity of the droplet and the resulting resistance to deformation at increased shear rates.

In the present study, the morphology of the reactively

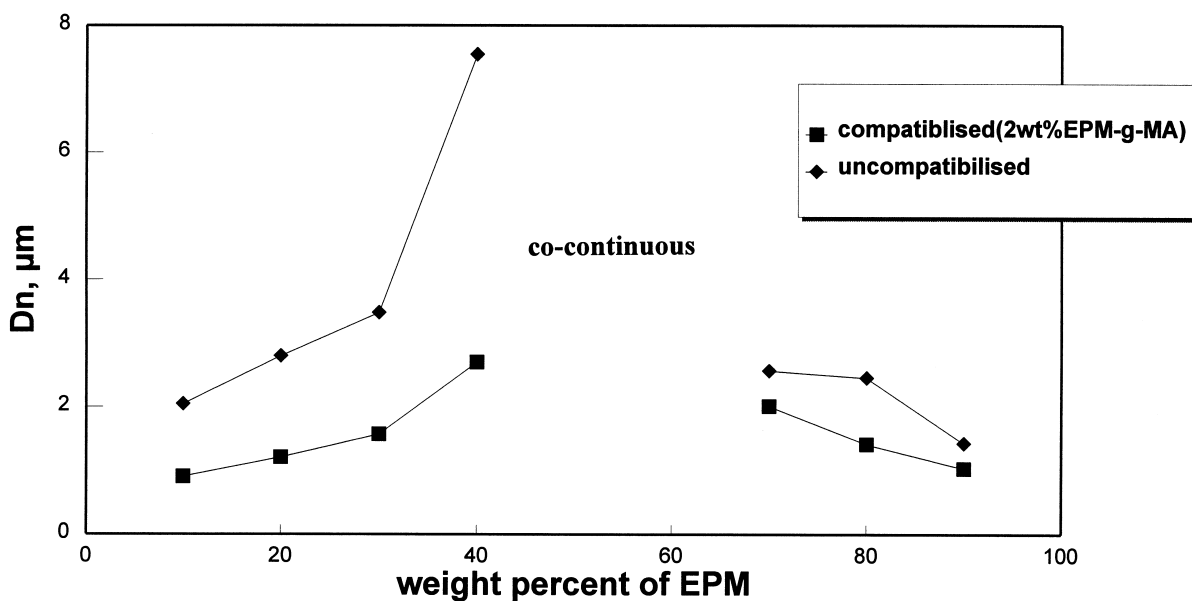


Fig. 4. Effect of blend ratio on number average domain diameter for uncompatibilised and reactively (2wt.% EPM-g-MA) compatibilised blends.

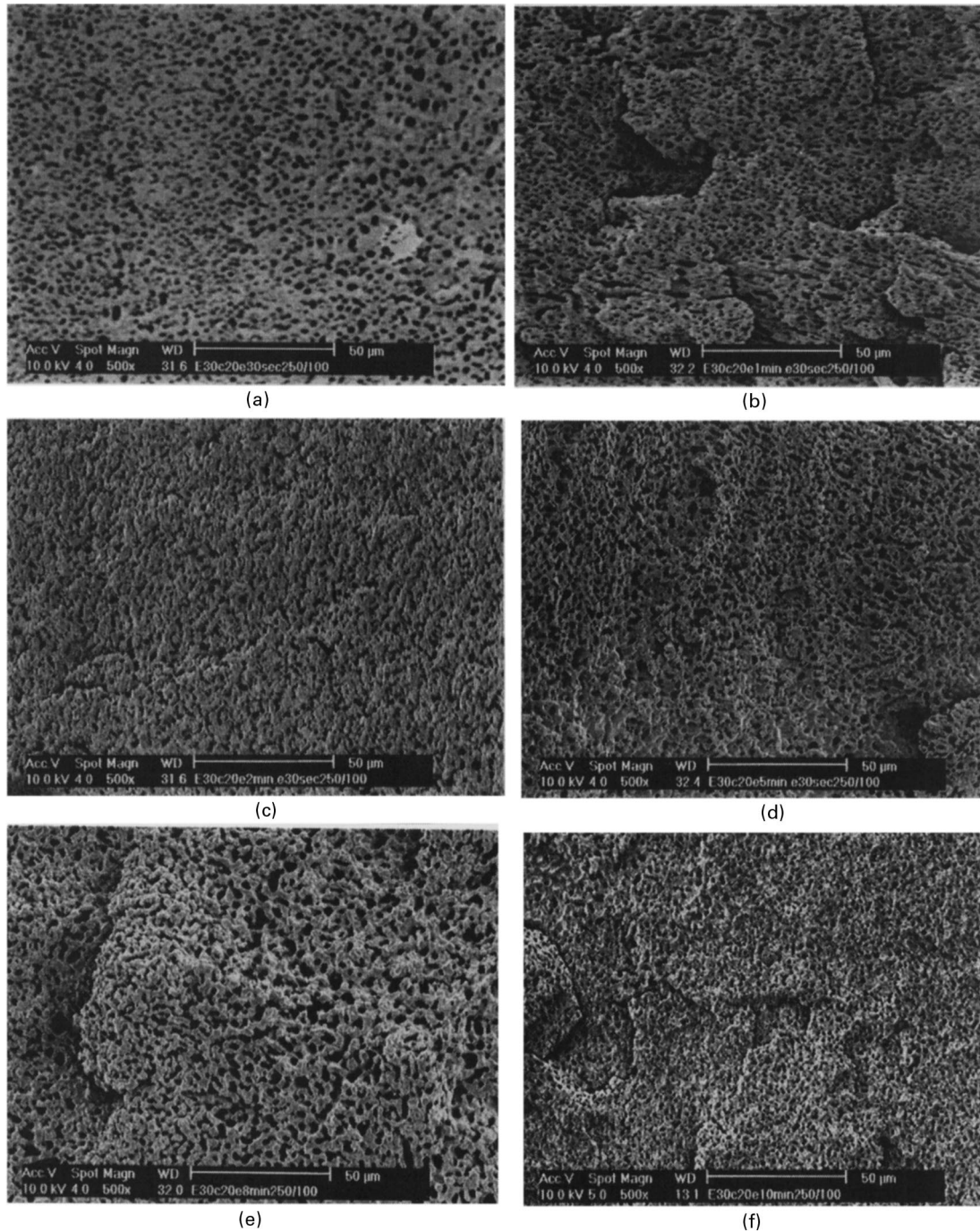


Fig. 5. SEM micrographs showing the morphology development during mixing of 30/70 EPM/nylon blend containing 20 wt.% of EPM-g-MA: (a) after 30 s, (b) after 1 min; (c) after 2 min; (d) after 5 min; (e) after 8 min; (f) after 10 min.

compatibilised blends over the entire composition range i.e., from 10/90 to 90/10 EPM/nylon can be understood from the SEM micrographs given in Figs. 3a–h. For blends having EPM concentration up to 60 wt.%, the rubber phase is extracted by boiling xylene. For other compositions 70/30, 80/20 and 90/10 EPM/nylon, the nylon phase was removed by formic acid. The morphology of the blends shows that at high nylon concentration, the rubber phase is preferentially dispersed as spherical inclusions in the low viscosity nylon

matrix up to 40 wt.% of its concentration. An interpenetrating co-continuous morphology is formed at 50 and 60 wt.% of EPM concentration followed by a phase inversion beyond 60 wt.% of rubber where the nylon phase is dispersed as spherical inclusions in the continuous EPM phase. This is in agreement with the studies of Denesi and Porter [44] who have shown that for blends with the same processing history, the morphology is determined by the melt-viscosity ratio and the composition. Generally, the least viscous

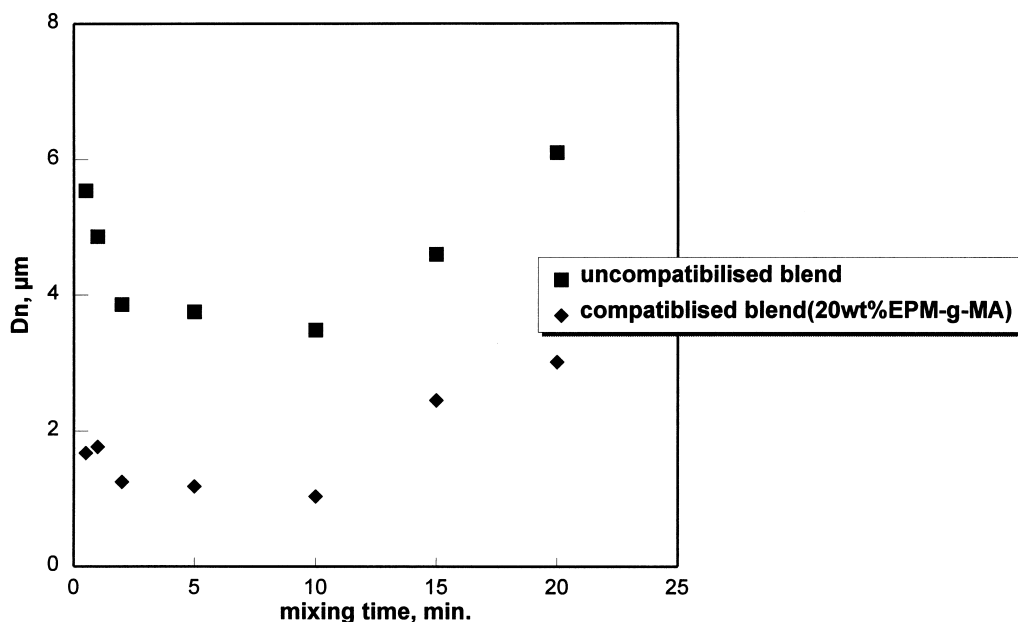


Fig. 6. Influence of mixing time on number average domain diameter for 30/70 EPM/nylon blend: uncompatibilised and compatibilised with 20 wt.% of EPM-g-MA.

component was observed from the continuous phase over a large composition range. Fig. 4 shows the number average domain diameter as a function of blend ratio for the uncompatibilised and the reactively compatibilised blend system. The variation in domain size with composition can be explained because of coalescence. It is important to note that the coalescence is more prominent when EPM is the dispersed phase. This is because of the fact that the dispersed EPM domains undergo coalescence easily caused by the high diffusional mobility in the low viscosity nylon phase. In contrast, as the viscosity of the EPM is very much higher than of nylon phase (Table 2), the diffusional mobility of nylon domains in the high viscosity EPM matrix is very low. This reduces the coalescence probability of the nylon domains. The influence of addition of compatibiliser on coalescence can be well understood from Fig. 4 where the progression of number average diameter as a function of blend composition is presented. It can be seen that the coalescence is substantially suppressed by the addition of the compatibiliser. Of course it is well known that one of the effects of the interfacial agent is to reduce the minor phase particle coalescence in the blend. However, it is important to note that the effect of interfacial agent on the suppression of coalescence becomes very significant only at higher concentration of the EPM phase. This is not an unexpected behaviour as the composition approaches the region of phase co-continuity at higher concentration of the EPM phase. Although there is substantial reduction in the particle size of the dispersed phase up on compatibilisation, it can be seen that the addition of compatibiliser does not have any influence on the location of the region of phase continuity. In both cases the co-continuity is observed between 40 and

70 wt.% of the EPM concentration. We have verified this further even at high concentration of the compatibiliser.

In order to understand the evolution of morphology, the morphology development was carefully followed as a function of mixing time. In fact the morphology development is the evolution of the blend morphology along an extruder from pellet-sized-particles to submicro domains which exist in the final blend. Many interesting studies have been reported in literature on the evolution of morphology as a function of time. The model experiments of Scott and Macosko [45,46] illustrate the mechanism of morphology development. According to them the initial stage of mixing involves shearing of the phases into ribbon or sheet structures followed by a shear and interfacial tension driven break-up of the structures into droplets. Most of the break-up in the dispersed size was found to occur in the very early stages of mixing. Figs. 5a–f show the morphology of the 30/70 blend EPM/nylon 6 containing 20 wt.% of EPM-g-MA, mixed for 0.5, 2, 4, 5, 8 and 10 min., respectively. The rotor speed and the mixing temperature were 100 rpm and 250°C, respectively. The number average domain diameter as a function of mixing time for the compatibilised and uncompatibilised blends are given in Fig. 6. Contrary to our expectation, the morphology development was so fast that within 30 s of mixing the morphology was already developed. Although the mixing was continued up to 20 min no major change in morphology could be observed up to 10 min. However upon prolonged mixing beyond 10 min. there was strong tendency for phase coarsening. In fact for the uncompatibilised system we could follow the morphology development as a function of time. In the uncompatibilised system the most significant domain

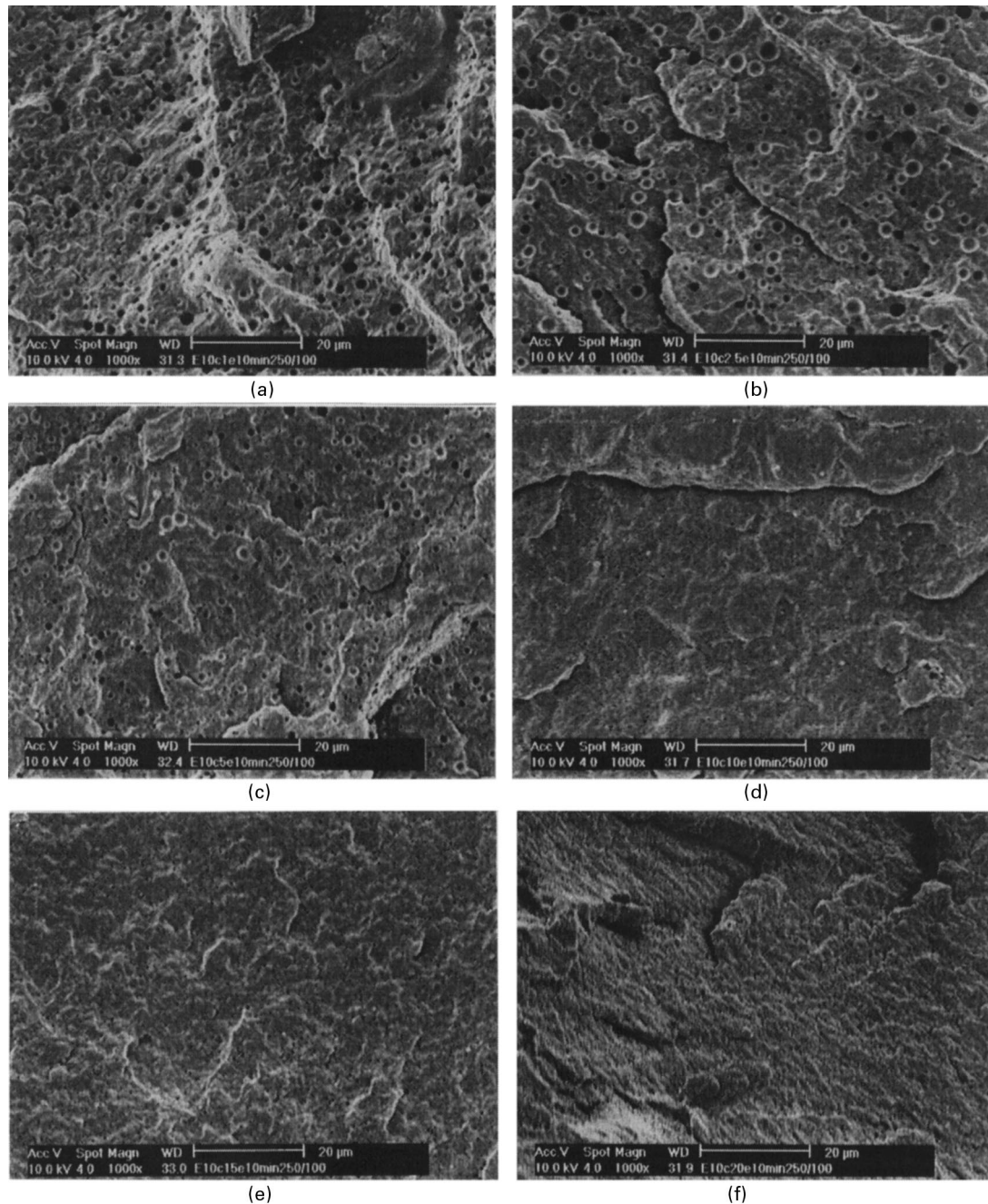


Fig. 7. SEM micrographs showing the morphology 10/90 EPM/nylon blends compatibilised with (a) 1 wt.% EPM-g-MA; (b) 2.5 wt.% EPM-g-MA; (c) 5 wt.% EPM-g-MA; (d) 10 wt.% EPM-g-MA; (e) 15 wt.% of EPM-g-MA; (f) 20 wt.% of EPM-g-MA.

break-up occurred within the first three minutes of the mixing time. This indicates that for the reactively compatibilised system one can achieve a stable morphology very fast. This is because of the fact that as the compatibiliser locates at the blend interface, the coalescence is substantially suppressed and the blend system attains a stable and equilibrium morphology very fast. The above results also indicate that the compatibilisation reaction is extremely fast so that this could be easily performed in the time scale of an industrial extruder. Additionally, it is important to note that

prolonged mixing can cause shear induced coalescence even in reactively compatibilised systems. We believe that upon continued mixing the compatibiliser can leave the interface because of the shear forces. Recently Dedecker and Groeninckx [47] have observed similar behaviour in the case of reactively compatibilised nylon 6/PMMA/SMA blends. Moreover, the nylon phase must have undergone severe thermal degradation on prolonged mixing at high temperature leading to a decrease in molecular weight. In fact we have observed a decrease in mixing torque on prolonged

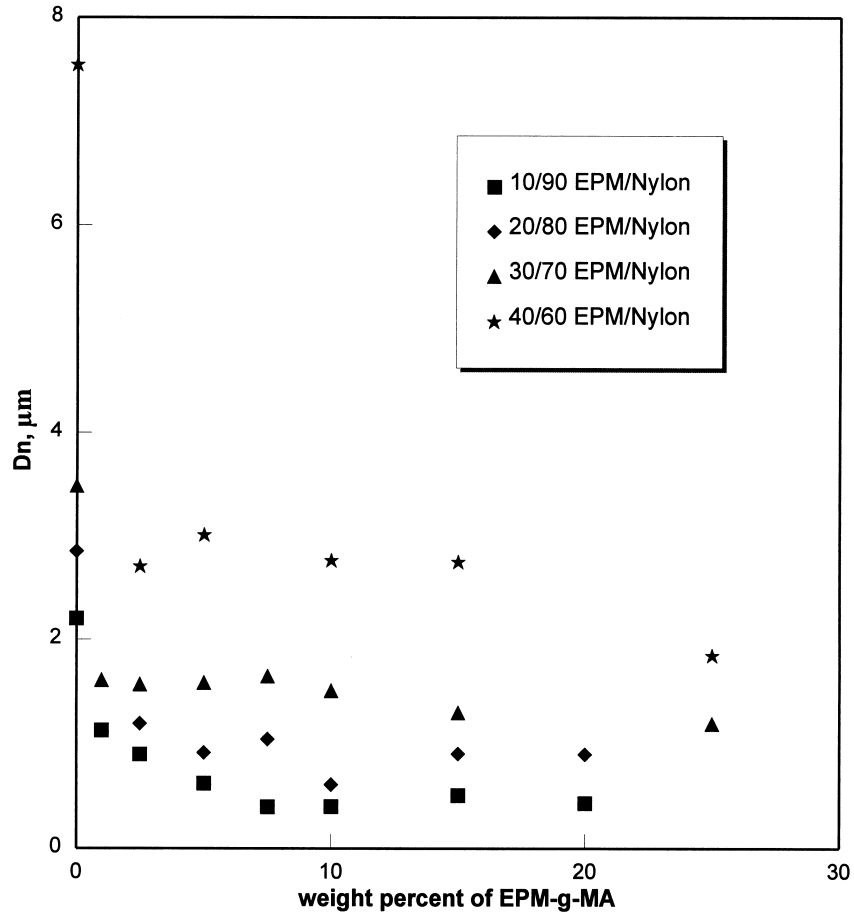


Fig. 8. Emulsification curves for EPM/nylon blends where EPM forms the dispersed phase.

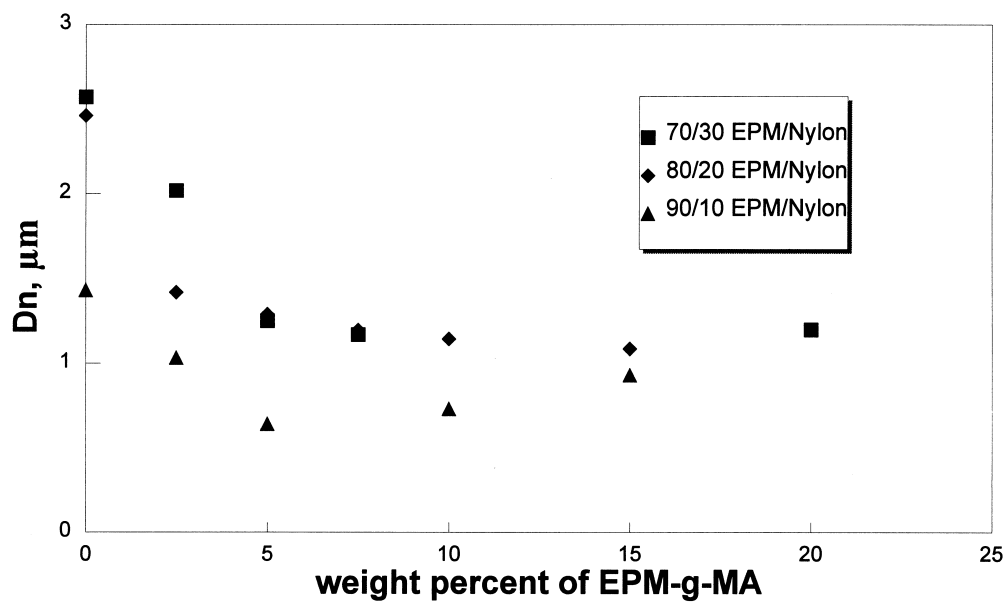


Fig. 9. Emulsification curves for EPM/nylon blends where nylon forms the dispersed phase.

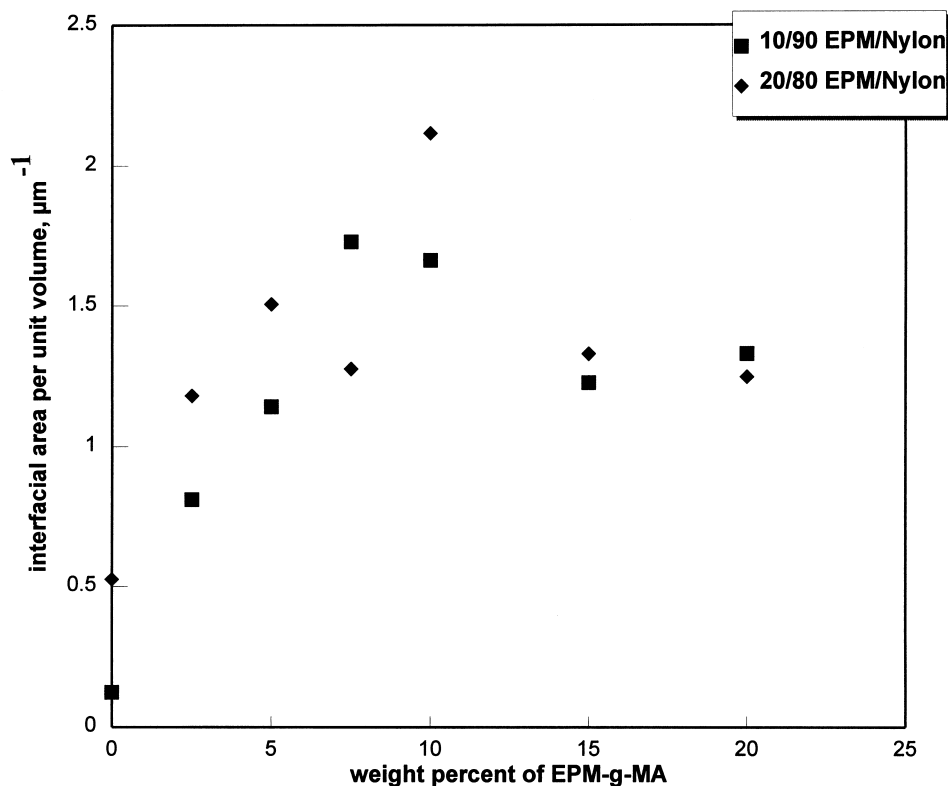


Fig. 10. Influence of EPM-g-MA concentration on the interfacial area per unit volume of 20/80 and 10/90 EPM/nylon blend.

mixing at longer times. This will of course contribute to a coarser morphology on account of rheological reasons.

3.4. Effect of concentration of EPM-g-MA compatibiliser on the morphology of the blends

The effect of EPM-g-MA as a compatibiliser on the morphology of the 10/90 EPM/nylon 6 blend is shown by the scanning electron micrographs in Fig. 7. Figs. 7a–f show the morphology of blends containing 1, 2.5, 5, 10, 15, 20 wt.% EPM-g-MA respectively. From the scanning electron micrographs it can be seen that the size of the dispersed EPM phase decreases with the addition of a few percent of EPM-g-MA followed by a levelling off at higher concentration. A similar behaviour was observed for all other blend compositions. The reduction in particle size with the addition of the functionalised EPM is because of the stabilisation of the blend morphology by the graft copolymer (EPM-g-MA) formed during melt-mixing. The formed graft copolymer reduces both the interfacial tension and thus the particle size, and the coalescence behaviour. In addition, the presence of the graft copolymer at the blend interface broadens the interfacial region through the penetration of the copolymer chain segments into the corresponding adjacent phases [47].

The number average domain diameter of the dispersed EPM and nylon phase in the blends was analysed as a function of compatibiliser concentration in Figs. 8 and 9,

respectively. These graphs are generally described as the so-called emulsification curves. Let us examine the 10/90 EPM/nylon blend in more detail. The number average domain size of the dispersed EPM phase in the uncompatibilised blend is 2.04 μm. From Fig. 8 it can be understood that a 45% reduction in domain size could be observed by the addition of only 1 wt.% of EPM-g-MA into the uncompatibilised blend. Addition of another 1.5 wt.% of the compatibiliser causes a further size reduction of only 20%. However, further addition of compatibiliser does not change the domain size that much and a very clear levelling off is observed. A similar levelling off was observed in all the blend compositions as can be seen from Figs. 8 and 9. The equilibrium concentration of EPM-g-MA at which the domain size levelled off can be considered as the so-called critical micelle concentration (CMC), i.e., the concentration at which micelles are formed. Generally the CMC is estimated from a plot of interfacial tension versus copolymer concentration. As the interfacial tension is directly proportional to the domain size, the estimation of CMC from the plot of domain size versus copolymer concentration is warranted [39,48]. This type of analysis has been extensively reported in the literature [49–52]. It is interesting to note that in most cases a 5 wt.% of the compatibiliser is sufficient for interfacial saturation. We have also estimated the interfacial area per unit volume of the blend as a function of the weight percent of EPM-g-MA (Fig. 10). It is interesting to note that the interfacial area per unit volume

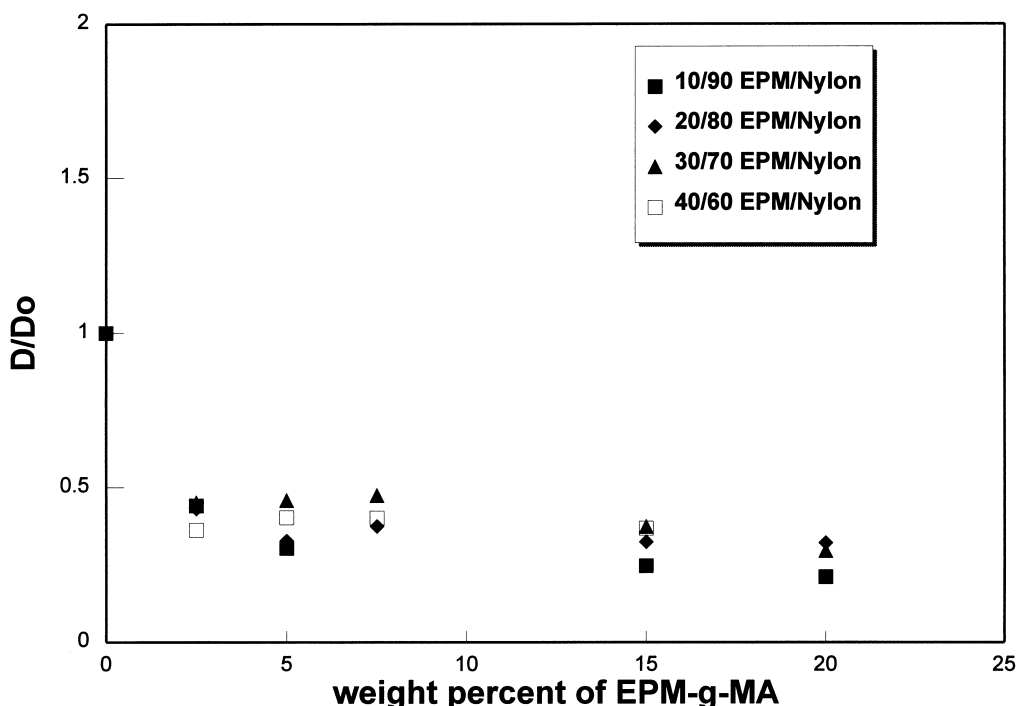


Fig. 11. Emulsification master curves.

increases with the addition of a few wt. percent of EPM-g-MA followed by a decrease at higher concentration. These observations clearly indicate that the interface is saturated.

Several interesting studies have been reported on the interfacial saturation in two phase polymer blends by the addition of compatibilisers. These include the studies of Fayt et al. [9], Thomas et al. [49] and Favis et al. [50,51], Park et al. [52] Quin et al. [53] and Spiros et al. [54]. Oommen, Nair and Thomas [49] reported that in poly(methyl methacrylate)/natural rubber (PMMA/NR) blends, at lower concentration of the graft copolymer (NR-g-PMMA), the dispersed phase size decreased linearly with increasing copolymer concentration, whereas at higher concentration it levelled off. In the case of natural rubber/polyethylene blends, a 5 wt.% of the compatibiliser (polyethylene-*b*-polyisoprene) was found to be sufficient for interfacial saturation [53]. The compatibilising action of poly(styrene-*b*-1,2 butadiene) in heterogeneous polystyrene/1,2 polybutadiene blends was reported by Spiros, Gancarz and Koberstein [54]. The interfacial tension reduced parallel with the copolymer addition up to a critical miscelle concentration (CMC) and thereafter levelled off at higher concentration. They suggested that beyond CMC further addition of the copolymer leads to micelle formation. Willis and Favis [50] reported that about 5% of ionomer is sufficient for polyolefin/polyamide blend system for interfacial saturation. Fayt, Jérôme and Teyssié [9,55] found equilibration in domain size by the addition of 0.5%–1% by weight of the compatibiliser. Recent studies of George et al. [15,56] and Park et al. [52] also report on the interfacial

saturation in reactively compatibilised polymer blends. The theoretical predictions of Noolandi and Hong [57–59] with respect to physical compatibilisation also showed that there is a critical concentration of the copolymer at which micelles are formed in the homopolymer phases.

All the reported experimental studies on the physical and reactive compatibilisation of immiscible polymer blends as well as our present study and the theoretical predictions of Noolandi and Hong suggest that a critical concentration of the compatibiliser is required to saturate the interface of binary polymer blends. Above this critical concentration, the compatibiliser may not modify the interface any more, but forms micelles in the bulk phase.

One can also explain the interfacial saturation point based on the Taylor's theory [27,28]. In the Taylor's theory the particle deformation and the critical Weber number, We , are related by the equation:

$$We = \gamma \eta_m D / 2Y. \quad (5)$$

On the addition of the compatibiliser, the interfacial tension decreases and there is a consequent particle break down (deformation). However, at a particular compatibiliser loading, there is a balance of interfacial tension and particle deformation. Thus there is a critical value of We below which no particle deformation occurs and hence a critical particle size. At this point the compatibiliser attains the highest possible interfacial area and therefore there must be a maximum quantity of compatibiliser required to saturate the blend interface.

We have further analysed whether or not the change in

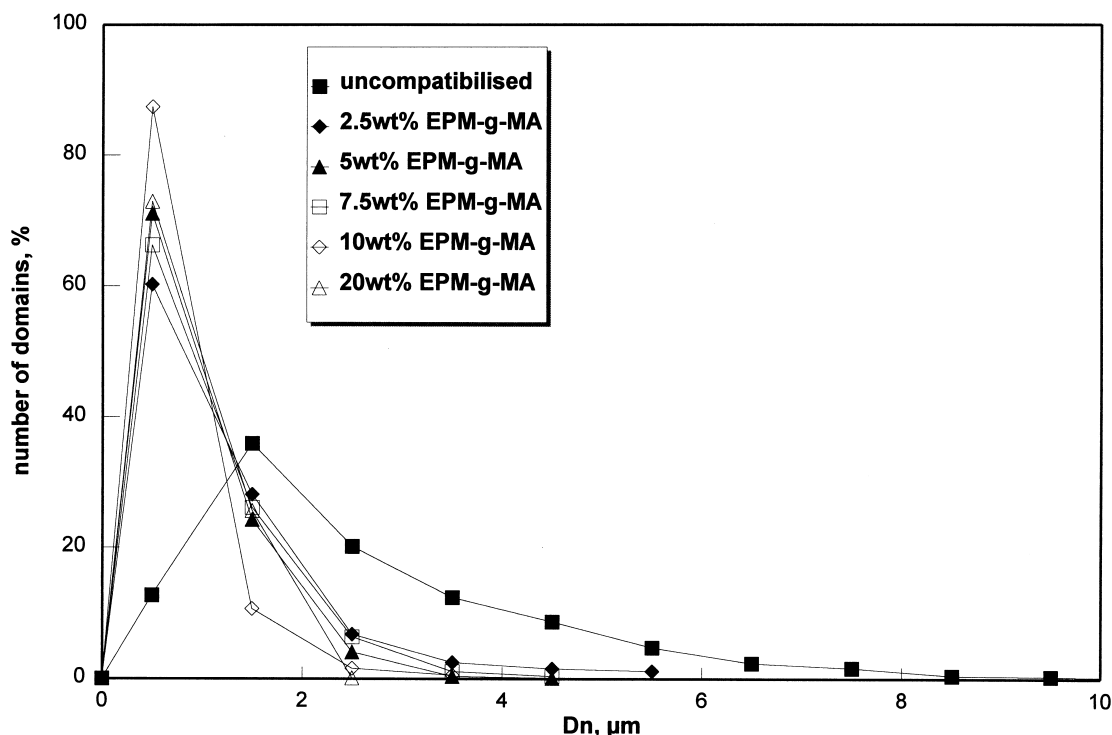


Fig. 12. Effect of EPM-g-MA concentration on the domain size distribution of 20/80 EPM/nylon blend.

domain size of the dispersed phase with increasing amount of EPM-g-MA for different blend compositions can be collapsed into one master curve when the reduced domain size (D_r) is considered as reported by Park and co-workers [52]. Here the reduced domain size, D_r , is defined by the ratio of the domain size (D) of each blend composition with EPM-g-MA to that of the respective blend composition without EPM-g-MA (D_0). The logic behind this analysis is based on the fact that the domain size of the dispersed phase of the blend (D) with EPM-g-MA can be considered by the following equation [52]:

$$D \sim [D_0(\chi, \dot{\gamma}, \eta_m, \eta_r, \phi \text{ etc}) Y_r(\phi_c, \chi)]. \quad (6)$$

In this equation D_0 depends on Flory's interaction parameter, χ ; shear rate, $\dot{\gamma}$; matrix viscosity, η_m ; viscosity ratio, η_r ; volume fraction of the component forming the dispersed phase in the blends, ϕ ; etc. The expression in D_0 in Eq. (6) can be obtained from Taylor's equation, as χ is related to interfacial tension. When the melt processing conditions are fixed at each ϕ , all parameters in D_0 do not change. However, the relative interfacial tension Y_r , which is the ratio of the interfacial tension (Y) of a blend with a compatibiliser to that of the respective blend without compatibiliser (Y_0), is certainly a function of the amount of compatibiliser, ϕ_c . If we assume that Y_r change very little with blend composition, the reduced diameter (D_r) has to be independent of composition. This definitely leads to a master curve. The plots of reduced domain size as a function of the weight percent of EPM-g-MA for the 10/90, 20/80, 30/70 and 40/60 EPM/nylon blends are given in Fig. 11.

Interestingly, all the curves unified into a single master curve regardless of the blend composition.

The formation of the master curve can be further explained based on the area occupied by the compatibiliser molecule at the blend interface. In fact the efficiency of the compatibiliser in reducing the domain size of the dispersed phase with the increasing concentration of the compatibiliser can be related to the interfacial area (Σ) occupied by the compatibiliser molecule at the blend interface. Let us consider a binary blend that contains a volume fraction ϕ_A of polymer A as spherical domains having a number average domain diameter of D_n in a matrix B. The total interfacial area per unit volume of the original blend is equal to $6\phi_A/D_n$. If each copolymer molecule occupies an area, Σ , at the interface, the mass, m , of the copolymer required to saturate unit volume of the blend interface is given by the following relation:

$$\Sigma = 6\phi_A M / m D_n D_n N_{av}, \quad (7)$$

where M is the molecular weight of the copolymer and N_{av} is Avogadro's number. The values of Σ for the 10/90, 20/80, 30/70 and 40/60 EPM/nylon blend compositions with 5 wt. percent of compatibiliser were 1.6, 2.13, 1.79, 1.23 nm², respectively. From this estimation it is clear that the area occupied by the compatibiliser molecule remains almost the same in all blend compositions. Therefore, one can argue that this is one of the reasons why all curves of D_r of different blend compositions collapsed into one master curve. In this context, we would like to indicate that for the estimation

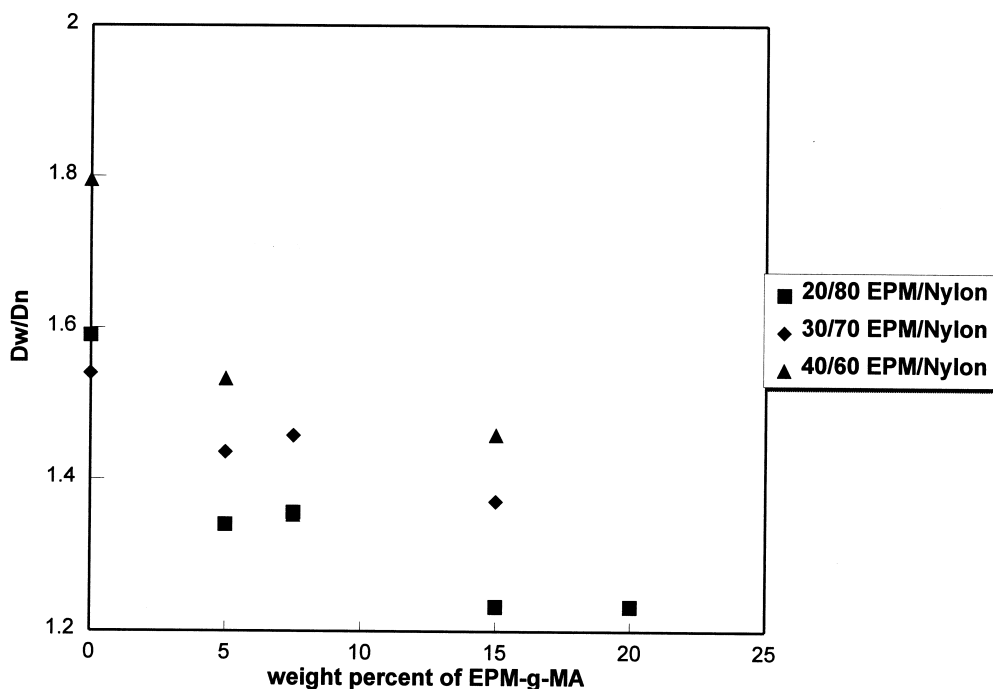


Fig. 13. Effect of weight percent of EPM-g-MA on the polydispersity index (D_w/D_n).

of the value of \sum we have assumed the molecular weight of the copolymer as 40,000, which is the number average molecular weight of EPM-g-MA. This is because of the fact that it is extremely difficult to know the exact molecular weight of the graft copolymer formed as a result of the reaction. It is important to mention that the error in estimating the molecular weight of the graft copolymer cancels out because of the m term in Eq. (7). Additionally, as the results of area calculations are used only to compare the different blend compositions, the conclusions made from this analysis are in no way affected by the error in estimating the molecular weight.

The influence of EPM-g-MA on the domain size distribution of the blends was analysed. The influence of the addition of EPM-g-MA on the domain size distribution of 20/80 EPM/nylon blend is presented in Fig. 12. It can be seen that the domain size distribution becomes narrower with increasing concentration of EPM-g-MA. This can be understood from the decreasing width of the distribution curve with increasing concentration of the compatibiliser. In fact the uncompatibilised blend contains a large number of bigger particles. The variation of the polydispersity index (D_w/D_n) as a function of EPM-g-MA is presented in Fig. 13. It is seen that the polydispersity index decreases with increasing concentration of EPM-g-MA followed by a levelling off tendency at higher concentration.

3.5. Comparison of the experimental compatibilisation data with theory

Noolandi et al. [57–59] and Leibler [60] have proposed

the thermodynamic theories concerning the compatibilising effect of copolymers in binary polymer blends. A general theory was proposed by Noolandi and Hong [57–59] for two immiscible homopolymers A and B diluted with a solvent in the presence of a diblock copolymer. The authors have derived the mean field equations for the fundamental probability distribution functions for the system. The polymer density profile in the interfacial region was obtained by solving the mean field equations by numerical analysis. The interfacial tension in these system was evaluated from free energy considerations. Their model was made based on the assumption that part of the copolymer that does not localise at the interface will be randomly distributed in the bulk of the homopolymer phases as micelles. In order to understand the importance of various contributions that influence the interfacial tension, numerical solutions of their model was used. For a symmetrical diblock copolymer, homopolymers of infinite molecular weight and a symmetric solvent, the various enthalpic and entropic contributions to the total free energy was predicted. Localisation of some of the block copolymers at the interface results in a lowering of the interfacial energy between the two immiscible homopolymers. In addition the interface region between the homopolymers is broadened leading to an increase of the turning back entropy of the polymer chains. The net effect of both contributions is to decrease the total free energy. Localisation of the copolymer however results in a decrease in the entropy and ultimately limits the amount of copolymer at the interface. The separation of the two blocks into the corresponding homopolymer phases gives a decrease in the energy of interaction of the two

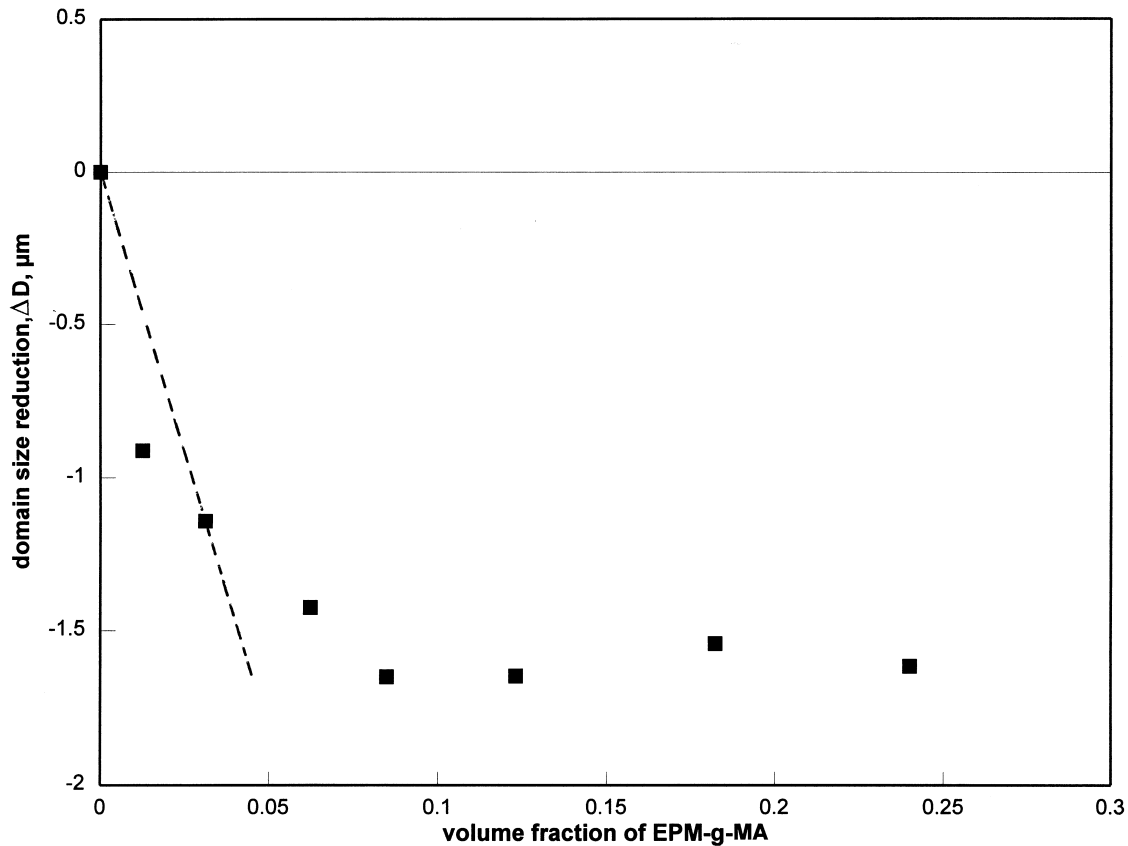


Fig. 14. Effect of volume fraction of EPM-g-MA on the domain size reduction of 10/90 EPM/nylon blend.

blocks with each as well as a large decrease in the interaction energy of the oriented blocks with the homopolymers, both with respect to the corresponding interactions when the copolymer is either of the bulk phases. The separation of the blocks and the consequent stretching of the blocks into corresponding homopolymers also cause a decrease of entropy. However, the main contributions to the interfacial tension reduction is the entropy loss of the copolymer that localises at the interface. The loss of conformational entropy of both the copolymer and homopolymer chains at the interface was shown to contribute very little to the interfacial tension reduction. An analytical expression for the interfacial tension reduction was derived by Noolandi and Hong by neglecting the loss of conformational entropy. According to their equation [57–59],

$$\Delta\gamma = d\Phi_c[(1/2\chi\Phi_p + 1/Z_c) - 1/Z_c \exp(Z_c\chi\Phi_p/2)], \quad (8)$$

where d is the width at half height of the copolymer profile reduced by the Kuhn statistical segment length, Φ_c the bulk copolymer volume fraction of the copolymer in the system, Φ_p the bulk volume fraction of polymer A or B, Z_c is the degree of polymerisation of the copolymer and χ is the Flory–Huggins interaction parameter between A and B segments. Numerical solutions based on the above

expression showed an exponential dependence of interfacial tension reduction on the block copolymer molecular weight. Noolandi and Hong further suggested that both copolymer molecular weight and concentration are equally important in reducing the interfacial tension. They noted that the interfacial tension surface is bounded by a critical micelle concentration curve as blocks of large molecular weight tend to form micelles in the bulk of the homopolymer phases. Therefore, the theoretical treatment of Noolandi and Hong is valid only for concentrations below CMC. For concentrations below CMC, the interfacial tension is expected to decrease linearly with copolymer concentration, whereas for concentrations higher than CMC a levelling off is expected.

Noolandi further suggested that in the absence of a solvent Eq. (8) reduces to

$$\Delta\gamma = d\Phi_c[1/2\chi + 1/Z_c - 1/Z_c \exp(Z_c\chi/2)]. \quad (9)$$

Although the theory was developed for the action of a symmetrical diblock copolymer, A-b-B, in incompatible binary blends (A/B), it can be very well applied to other systems too where the compatibilising action is not strictly by the addition of block copolymers [49,52]. As the interfacial tension reduction is directly proportional to the particle size reduction at low volume fraction of the dispersed

Coalescence = collision and subsequent merging of droplets

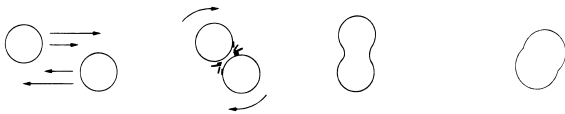


Fig. 15. Schematic representation of the coalescence behaviour.

phase, as suggested by Wu [39], it can be argued that

$$\Delta D = Kd\Phi_c[1/2\chi + 1/Z_c \exp(Z_c\chi/2)], \quad (10)$$

where K is a proportionality constant.

The plot of domain size reduction as a function of the volume fraction of the EPM-g-MA for the 10/90 EPM/nylon blend is shown in Fig. 14. It can be seen that at low EPM-g-MA concentration (below CMC), ΔD decreases almost linearly with increasing EPM-g-MA volume fraction, whereas at higher concentration (above CMC) a levelling off is observed, in agreement with the predictions of Noolandi and Hong. In this analysis, it is very important to mention that in the 10/90 EPM/nylon blend, it is believed that the added EPM-g-MA reacts almost completely with the amino end group of nylon. In fact in 10/90 EPM/nylon blend there are large number of amino groups to react with the

relatively few anhydride groups present (0.6 mol.% only) in EPM-g-MA. Therefore, a proportionate amount of EPM-g-nylon must have been formed as a result of the reaction. As the melt viscosity of the nylon phase is very low, the formed graft copolymer can easily diffuse towards the blend interface. Similar observations regarding the mobility of graft copolymer formed during reactive compatibilisation have been recently reported by Dedecker and Groeninckx in the case of reactively compatibilised nylon6/PMMA/SMA blend systems [47]. Therefore, the plotting of EPM-g-MA in the X axis of Fig. 14 instead of EPM-g-nylon is justified.

3.6. Phase coarsening (coalescence) of molten blend under quiescent conditions

Coalescence or phase coarsening in Newtonian systems has been a topic of considerable research interest for the last several years. While collision and coalescence probability can be predicted with a reasonable degree of certainty in Newtonian systems, only crude estimates are available in the case of viscoelastic systems like polymer blends. The course of coalescence in a molten quiescent polymer blend is often described as a four step process. The first step

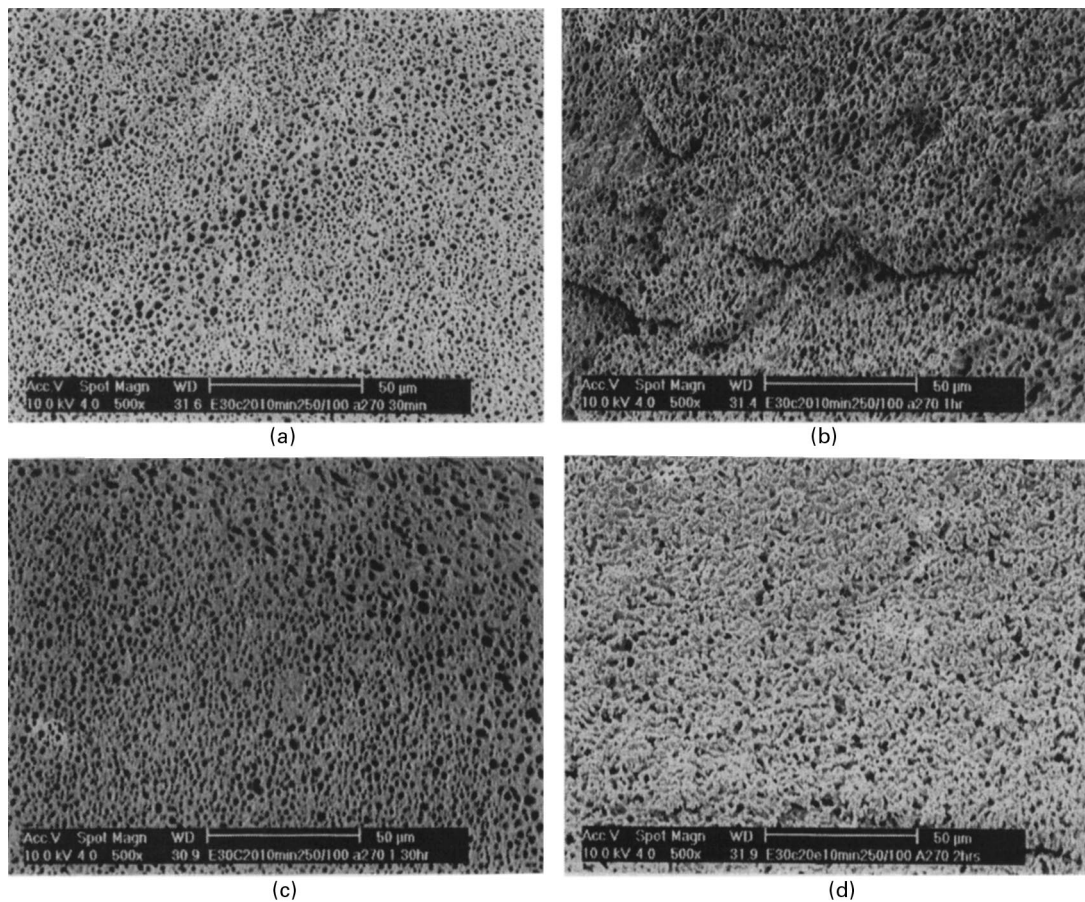


Fig. 16. SEM micrographs showing the evolution of the morphology as a function of annealing time for 30/70 EPM/nylon blend containing 20 wt.% of EPM-g-MA at a temperature of 270°C: (a) 30 min. annealing, (b) 60 min. annealing, (c) 90min. annealing, (d) 120 min. annealing.

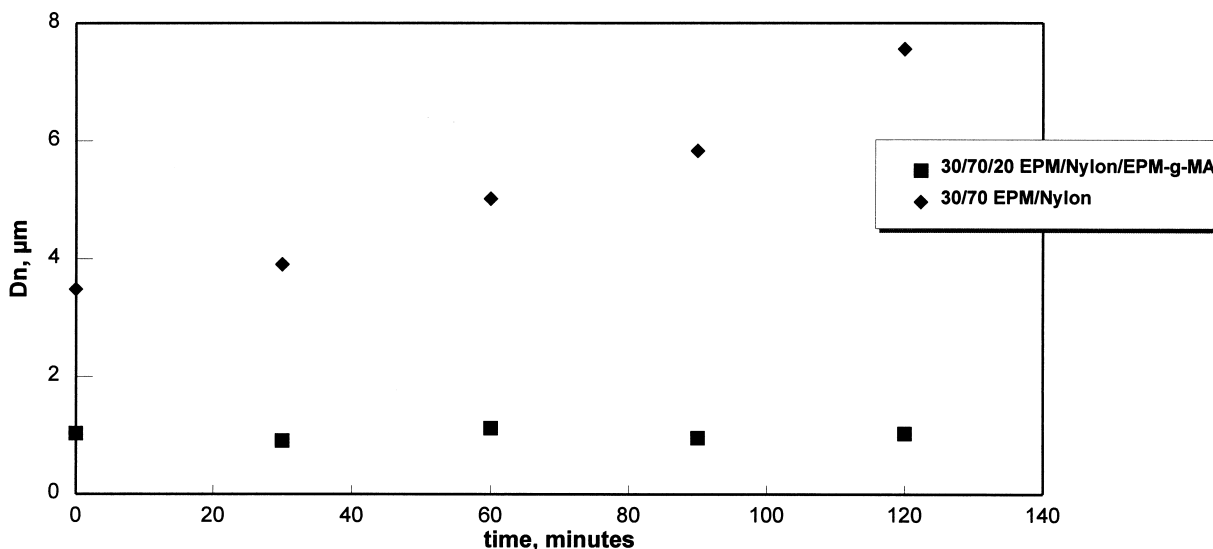
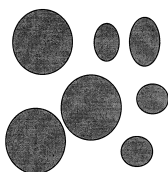


Fig. 17. Effect of annealing on the number average domain diameter of uncompatibilised and compatibilised (20 wt.% EPM-g-MA) 30/70 EPM/nylon blend.

concerns the approach of the droplets as a result of the flow field or Brownian motions in a quiescent blend. It is to be noted that the higher the concentration of the dispersed phase, the closer the droplets, and the higher the probability of collision. In practice the first step is important only in systems where the volume fraction of the dispersed phase is lower than 10%. At high concentration of the dispersed phase, many droplets practically touch each other because the percolation threshold for a system of spheres is at 15.6 volume percent. The second step for coalescence is the so-called deformation of the droplets. In the third step the matrix film ruptures at the thinnest spot by the formation of a hole. Finally the drops merge together to form one single droplet. This is schematically presented in Fig. 15.

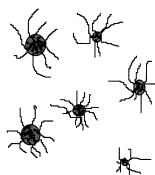
In the present study the phase coarsening of the quiescent blend was followed under isothermal conditions at an annealing temperature of 270°C as a function of time for the 30/70 EPM/nylon blend containing 20 wt.% of EPM-g-MA. The purpose of this experiment was to follow the

Uncompatibilised



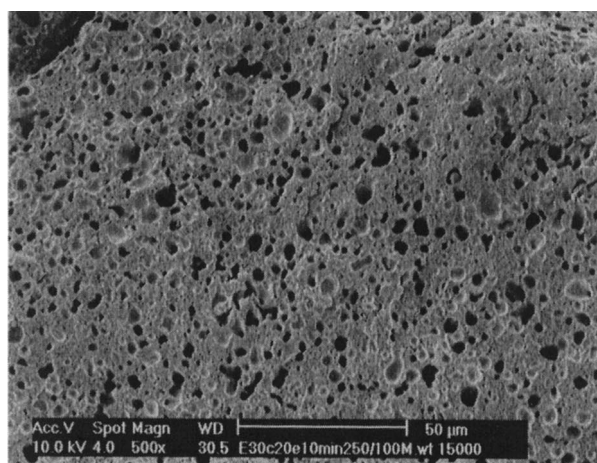
narrow interface
high interfacial tension
larger domain size
highly mobile interface

Compatibilised

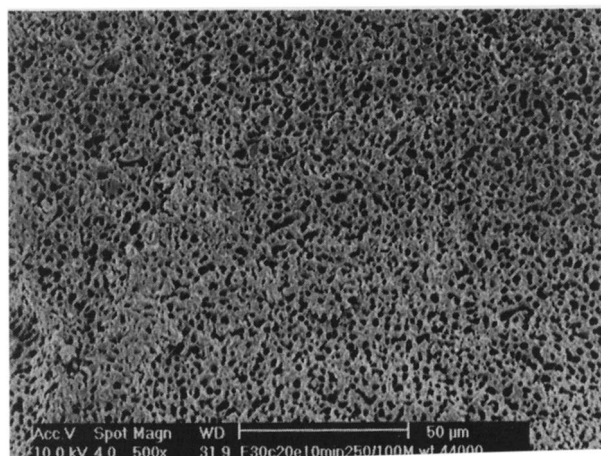


broad interface
low interfacial tension
smaller domain size
less mobile interface

Fig. 18. Schematic model illustrating the interface of uncompatibilised and reactively compatibilised blends.



(a)



(b)

Fig. 19. SEM micrographs showing the morphology of 30/70 EPM/nylon blend containing 20 wt.% of EPM-g-MA as a function of the molecular weight of the nylon matrix: (a) $M_w = 15\,000$; (b) $M_w = 44\,000$.

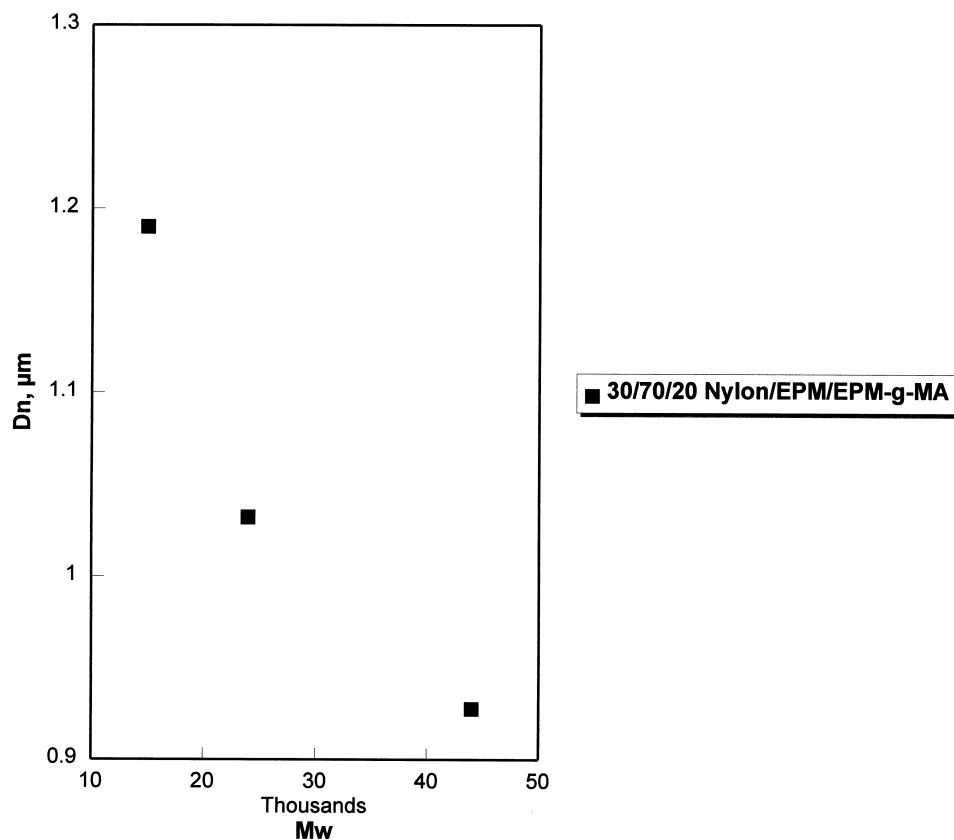


Fig. 20. Effect of molecular weight of nylon on the number average domain diameter of 30/70 EPM/nylon blend containing 20 wt% EPM-g-MA.

evolution of the morphology as a function of time. The morphologies of the compatibilised 30/70 EPM/nylon blend annealed for 30, 60, 90 and 120 min are given in Figs. 16a–d, respectively. It can be seen from Fig. 17 that the number average domain diameter is unaffected by annealing in the case of compatibilised blends. However in the case of the uncompatibilised blends, the domain size increases dramatically as a function of time [61]; the rate of growth was found to be much faster at longer times. These observations clearly indicate that the graft copolymer stabilises the morphology against coalescence. This has been further presented with the aid of a schematic model given in Fig. 18. In the case of compatibilised blends, the copolymer is located at the blend interface and a shell of block copolymer is formed around the dispersed phase. This in fact leads to a broad, stable and less mobile interface which can resist coalescence.

3.7. Influence of the molecular weight of nylon matrix on dispersed phase size

The morphology of 30/70 compatibilised EPM/nylon blend as a function of molecular weight of nylon matrix phase is given in Figs. 19a,b. The number average domain diameter is presented as a function of molecular weight of nylon in Fig. 20. It can be understood that as the molecular

weight of nylon increases, more finer domain size is achieved. The molecular weight effect on blend morphology can be explained based on the fact that as the molecular weight of the matrix increases, the viscosity of the matrix increases and this leads to the finer distribution of the minor phase in the major one. The polydispersity was also found to decrease with increasing molecular weight. The influence of molecular weight of nylon matrix on the morphology and properties of various nylon/rubber blends has been studied by Paul and co-workers [62]; they observed a decrease in domain size of the dispersed phase with increasing molecular weight.

3.8. Fracture surface morphology and extent of interface adhesion

It has already been reported that in the case of immiscible blends comprised of a crystalline and amorphous component, depending on whether the crystalline material is the dispersed phase or matrix, high levels of voiding or good apparent contact respectively could be obtained [63]. In view of this, we have examined the fracture surface morphology of 30/70 and 70/30 EPM/nylon blends containing 2.5 wt.% of EPM-g-MA (Fig. 21). No signs of interfacial voiding could be observed. The dispersed phase is well bonded with the matrix. In contrast, the fracture

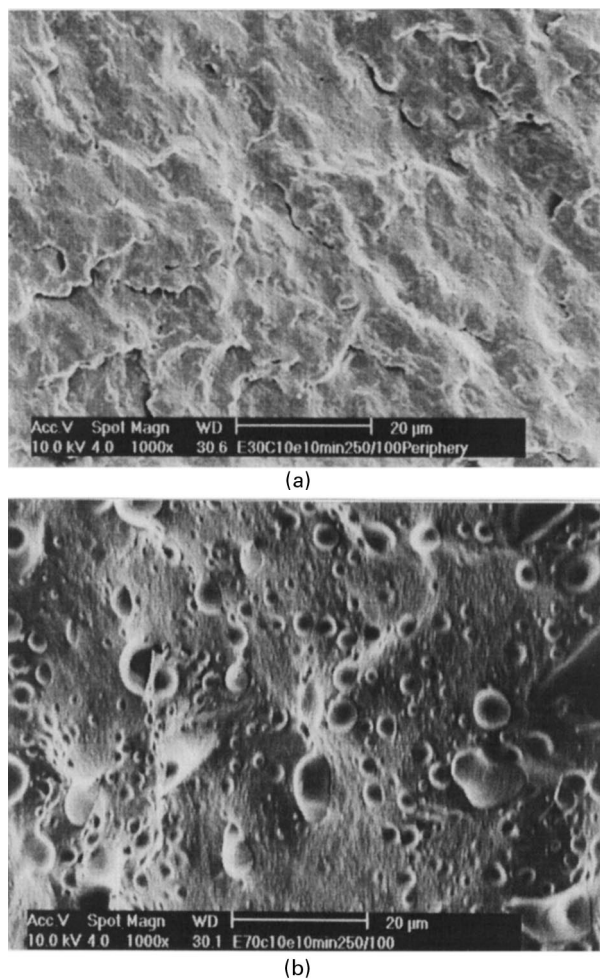


Fig. 21. SEM micrographs showing the fracture surfaces: (a) 30/70 EPM/nylon blend containing 2.5 wt.% of EPM-g-MA, (b) 70/30 EPM/nylon blend containing 2.5 wt.% of EPM-g-MA.

surfaces of uncompatibilised 30/70 and 70/30 blends showed high extent of void formation and debonding [61]. These observations clearly indicate that compatibilisation enhances interfacial adhesion between the phases.

3.9. Effect of mode of addition of the compatibiliser

In order to study the influence of mode of addition of EPM-g-MA, the blending operations were carried out in four different ways: These include:

- (i) Nylon, EPM rubber and EPM-g-MA were added together into the extruder and then mixed
- (ii) Both nylon and EPM were preblended for three minutes and then EPM-g-MA was added into the blend
- (iii) EPM-g-MA was preblended with the minor EPM phase for 3 min (EPM master batch) and then mixed with the nylon phase
- (iv) EPM-g-MA was preblended with the major continuous nylon phase for 3 min (nylon master batch) and then mixed with the EPM minor phase.

Table 3

Effect of order of addition of compatibiliser on the morphology of 20/80/10 EPM/Nylon/EPM-g-MA blend

Mode of addition	$D_n(\mu\text{m})$	$D_w(\mu\text{m})$	D_w/D_n
Added into blend	1.02	1.54	1.50
Nylon masterbatch	2.03	3.42	1.68
EPM masterbatch	0.50	0.620	1.24
Mixed together (simultaneous)	0.61	0.92	1.50

The morphology of the 20/80 EPM/nylon blend containing 10 wt.% of EPM-g-MA for the case (i), (ii), (iii); and (iv) are given in Figs. 22a–d respectively. The results are presented in Table 3. It is interesting to note that the most finer and uniform dispersion is obtained when the EPM-g-MA was preblended with the minor EPM phase. The size of the domains increases in the order case (iii) < case (i) < case (ii) < case (iv); case (iv) was the worst. This has been further explained in Fig. 23 with a schematic model. In fact a two-step mixing process in which the EPM-g-MA is mixed with the EPM phase (EPM master batch) gives more opportunity for the EPM-g-MA to diffuse towards the blend interface. In this method of mixing, the EPM-g-MA is forced to be at the blend interface. This will lead to a situation where the EPM-g-MA can react with the amino end group of nylon at the interface and the resulting graft copolymer will be easily located at the blend interface. Interestingly the polydispersity was lowest in this case (Table 3). In contrast, when the EPM-g-MA is pre-mixed with the nylon phase at high temperature (nylon master batch), the graft copolymer is already generated as result of the reaction between the amino end group of nylon and MA group of EPM-g-MA. This graft copolymer has to diffuse into the blend interface during the final mixing with the EPM rubber. It is believed that only a very small fraction of the graft copolymer will be able to reach the interface in such a situation. Most of the graft copolymer will be located in the bulk nylon phase where they will give rise to micellar aggregation as depicted in Fig. 23d. Therefore this mode of mixing, (iv) gives a coarser morphology. We would like to further comment that in an industrial scale the first method (i) i.e.; simultaneous addition all the components together into the extruder is the most feasible one which in fact gives a morphology comparable to the situation in case (iii).

4. Conclusions

The influence of reactive compatibilisation on the morphology of immiscible EPM/nylon 6 blends was investigated as a function of composition, mixing time, temperature and annealing of the blends under quiescent state. The morphology of the compatibilised blends was examined over the entire composition range. The morphology indicated a two-phase structure in which the high viscosity

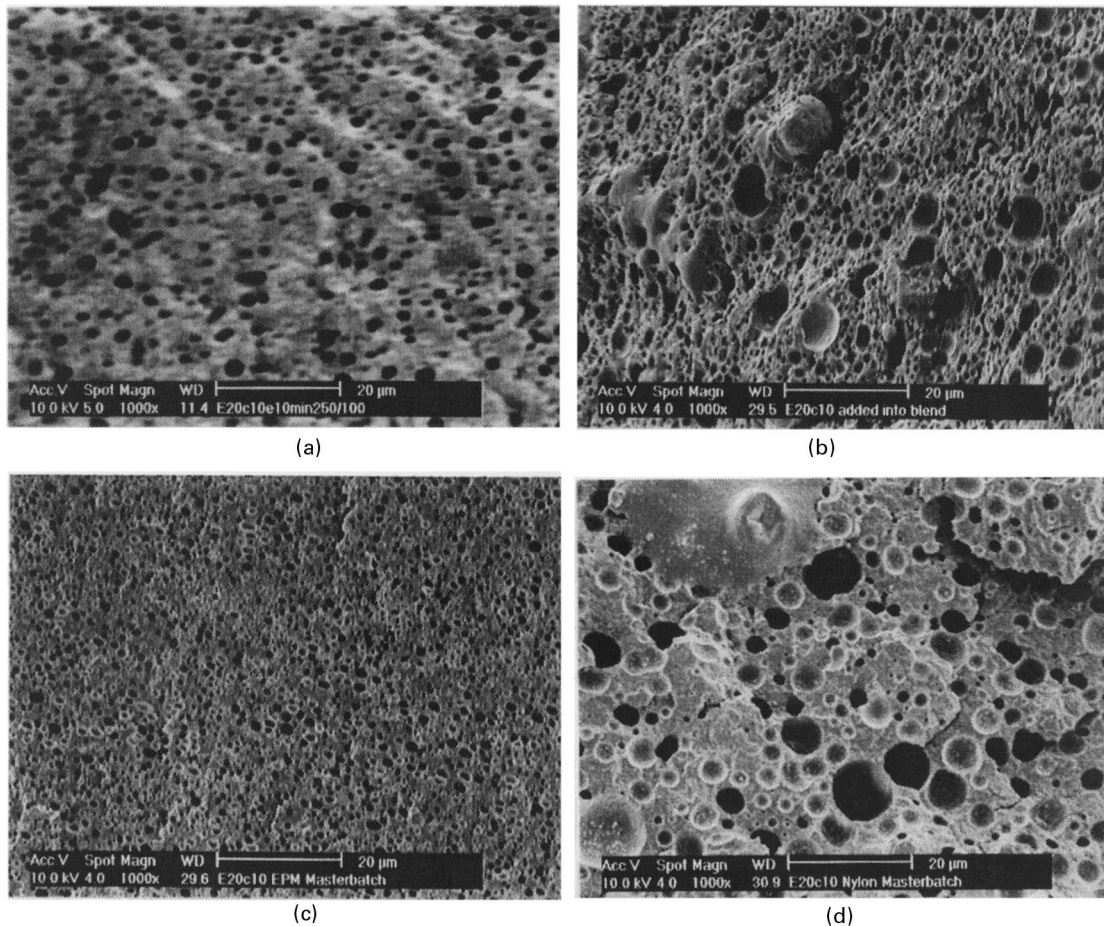


Fig. 22. SEM micrographs showing the influence mode of addition the morphology of 20/80 EPM/nylon blend containing 10 wt.% of EPM-g-MA: (a) nylon, EPM rubber and EPM-g-MA were added together into the extruder and then mixed, (b) both nylon and EPM were preblended for three minutes and then EPM-g-MA was added into the blend, (c) EPM-g-MA was preblended with the minor EPM phase for 3 min (EPM master batch) and then mixed with the nylon phase, (d) EPM-g-MA was preblended with the major continuous nylon phase for 3 min (nylon master batch) and then mixed with the EPM minor phase.

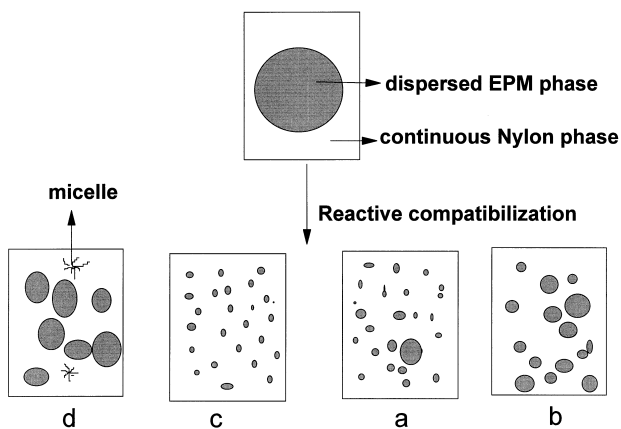


Fig. 23. Schematic models illustrating the mode of mixing on blend morphology: (a) mixing all together (simultaneous addition), (b) added into blend, (c) EPM masterbatch, (d) nylon masterbatch.

EPM phase was dispersed as domains in the continuous low viscosity nylon matrix up to 40 wt.% of the EPM concentration. An interpenetrating co-continuous phase morphology was obtained for 50/50 and 60/40 EPM/nylon compositions. At high EPM concentrations (>60 wt.%), the nylon phase was dispersed as domains in the continuous EPM matrix. The size of the dispersed phase was found to increase marginally with the increasing concentration of that phase which is associated with coalescence. The coalescence was predominant only at higher concentration of the dispersed phase. The coalescence behaviour was much less prominent in the reactively compatibilised blends as compared to the uncompatibilised blends. It was observed that the region of phase co-continuity was not affected by the presence of the compatibiliser. The morphology development as a function of the mixing time indicated that the system attains a stable morphology within 30 s of mixing. Extending the time of mixing beyond 30 s has little effect on the morphology; however, prolonged mixing beyond 10 min. led to shear induced coalescence.

The domain size of the dispersed phase in the blend

decreases with the increasing concentration of the compatibiliser followed by a levelling off at higher concentrations, which is an indication of interfacial saturation. The reduced domain size as a function of compatibiliser content collapsed into a single master curve for different blend compositions. This was accounted for by the fact that the area occupied by a compatibiliser molecule at the interface is the same in all the blends irrespective of the blend composition. The theories of Noolandi and Hong predict a linear decrease of interfacial tension with the increasing compatibiliser volume fraction for concentrations less than CMC. Considering the fact that the interfacial tension is directly proportional to the domain size at low volume fraction of the dispersed phase, it is demonstrated that the experimental data are in good agreement with the predictions of Noolandi and Hong. Isothermal annealing experiments at high temperature were performed on the blend samples. No phase coarsening could be observed upon isothermal annealing in the case of compatibilised blends. In the reactively compatibilised blends, the size of the dispersed EPM phase was found to decrease with the increasing molecular weight of the nylon matrix phase. The fracture surface morphology of the reactively compatibilised blends indicated excellent adhesion between the phases, as evidenced by the absence of micro-voids irrespective of the nature of the dispersed phase (EPM or nylon). Finally, the mode of addition of the compatibiliser indicated that the finest morphology is attained by preblending the EPM-g-MA in the minor EPM phase and then mixing with the continuous nylon phase.

Acknowledgements

The authors are indebted to the Research Council of the KU Leuven for a fellowship to one of them (S.T), and to the Fund for Scientific Research- Flanders (Belgium) for the financial support given to the MSC laboratory.

References

- [1] Walker BM, editor. Handbook of thermoplastic elastomers, New York: Van Nostrand Reinhold, 1979.
- [2] De SK, Bhowmick AK, editors. Thermoplastic elastomers from rubber-plastic blends, Chichester, UK: Ellis Horwood, 1990.
- [3] Macosko CW, Guégan P, Khandpur AK, Nakayama A, Maréchal P, Inoue T. *Macromolecules* 1996;29:5590.
- [4] Favis BD. *J Appl Polym Sci* 1990;39:285.
- [5] Sundararaj U, Macosko CW. *Macromolecules* 1995;28:2647.
- [6] Paul DR, Newman S, editors. *Polymer blends*, New York: Academic Press, 1978.
- [7] Molau GE. *J Polym Sci* 1965;A3:4235.
- [8] Riess G, Kohler J, Tournut C, Bandert A. *Makromol Chem* 1967;101:58.
- [9] Fayt R, Jérôme R, Teyssié Ph. *Polym Eng Sci* 1987;27:328.
- [10] Barentsen WM, Heikens D, Piet P. *Polymer* 1974;15:119.
- [11] Paul DR, Barlow GW. *ACS Adv Chem Ser* 1979;176:315.
- [12] Ide F, Hasegawa A. *J Appl Polym Sci* 1974;18:963.
- [13] Baker WE, Saleem M. *Polymer* 1987;28:2057.
- [14] Greco R, Malinconico M, Martuscelli E, Ragosta E, Scarinzi G. *Polymer* 1987;28:115.
- [15] George S, Joseph R, Varghese KT, Thomas S. *Polymer* 1995;36:4405.
- [16] Fakirov S, Evstatiev M, Petrovich S. *Macromolecules* 1993;26:5219.
- [17] Eersels KLL, Aerdt AM, Groeninckx G. *Macromolecules* 1996;29:1046.
- [18] Xanthos M. *Polym Eng Sci* 1988;28:1392.
- [19] Majumdar B, Keskkula H, Paul DR. *Polymer* 1994;35:3164.
- [20] Liu NC, Baker WE. *Adv Polym Tech* 1992;11:249.
- [21] Brown SB. Reactive extrusion, a survey of chemical reactions of monomers and polymers during extrusion processing. In: Xanthos M, editor. *Reactive extrusion principles and practice*. Munich: Hanser, ch. 4, 1992:75.
- [22] Martuscelli E, Riva F, Sellitti C, Silvestre C. *Polymer* 1985;26:270.
- [23] Cimmino S, D'orazio L, Greco R, Maglio G, Malinconico M, Mancarella C, Martuscelli E, Palumbo R, Ragosta G. *Polymer* 1994;24:48.
- [24] Dijkstra K, van der Wal A, Gaymans RJ. *J Mater Sci* 1994;29:3489.
- [25] Dijkstra K, Laak ter J, Gaymans RJ. *Polymer* 1994;35:315.
- [26] van der Velden G, Nelissen H, Veermans T. *Acta Polym* 1996;47:161.
- [27] Taylor GI. *Proc R Soc London* 1932;A 138:41.
- [28] Taylor GI. *Proc R Soc London* 1934;A 146:501.
- [29] Bartok W, Manson SG. *J Colloid Sci* 1958;13:393.
- [30] Bartok W, Manson SG. *J Colloid Sci* 1959;14:13.
- [31] Rumscheidt FD, Manson SG. *J Colloid Sci* 1961;16:238.
- [32] Torza S, Cox RC, Manson SG. *J Colloid Interface Sci* 1972;38:395.
- [33] Karan HJ, Bellinger JC. *Ind Eng Chem Fundam* 1986;167:241.
- [34] Grace HP. *Chem Eng Commun* 1982;14:225.
- [35] Acrivos A, Lo TS. *J Fluid Mech* 1978;86:641.
- [36] Chin HB, Han CD. *J Rheol* 1979;23:557.
- [37] Chin HB, Han CD. *J Rheol* 1980;24:1.
- [38] van Oene HJ. *J Colloid. Interface Sci* 1972;40:448.
- [39] Wu S. *Polym Eng Sci* 1987;27:335.
- [40] Huneault MA, Shi ZH, Utracki LA. *Polym Eng Sci* 1995;35:115.
- [41] Roland CM, Bohm GGA. *J Polym Sci, Polym Phys Ed* 1984;22:79.
- [42] Oshinski AJ, Keskkula H, Paul DR. *Polymer* 1996;37:4891.
- [43] Serpe G, Jarrin J, Dawans F. *Polym Eng Sci* 1990;30:553.
- [44] Denesi S, Porter RS. *Polymer* 1978;19:448.
- [45] Scott CE, Macosko CW. *Polym Bull* 1991;26:341.
- [46] Scott CE, Macosko CW. *Polymer* 1994;25:5422.
- [47] Dedecker K, Groeninckx G. *Polymer* 1998;39:4985–4993.
- [48] Thomas S, Prud'homme RE. *Polymer* 1992;33:4260.
- [49] Oommen Z, Nair MRG, Thomas S. *Polym Eng Sci* 1996;36:151.
- [50] Willis JM, Favis BD. *Polym Eng Sci* 1990;30:1073.
- [51] Cigana P, Favis BD, Jérôme R. *J Polym Sci Polym Phys* 1996;34:1691.
- [52] Kim SJK, Kim S, Park CE. *Polymer* 1997;38:2155.
- [53] Quin C, Yin J, Huang B. *Polymer* 1990;31:663.
- [54] Spiros HA, Gancarz I, Koberstein JT. *Macromolecules* 1989;22:1449.
- [55] Fayt R, Jérôme R, Teyssié Ph. *J Polym Sci Polym Phys Ed* 1982;20:2209.
- [56] George J, Varghese KT, Joseph JR, Thomas S. *J Appl Polym Sci* 1995;57:449.
- [57] Noolandi J. *Polym Eng Sci* 1984;24:70.
- [58] Noolandi J, Hong KM. *Macromolecules* 1982;15:482.
- [59] Noolandi J, Hong KM. *Macromolecules* 1984;17:1531.
- [60] Leibler L. *Macromolecules* 1982;15:1283.
- [61] Thomas S, Groeninckx G. *J Appl Polym Sci*, in press.
- [62] Oshinski AJ, Keskkula H, Paul DR. *Polymer* 1996;37:4919.
- [63] Leclair A, Favis BD. *Polymer* 1996;37:4723.